Symmetries of the eigenstates in an anisotropic photonic crystal

G. Alagappan and X. W. Sun*
School of Electrical and Electronical Engineering, Nanyang Technological University, Nanyang Avenue, Singapore 639798, Singapore

H. D. Sun
School of Physical and Mathematical Sciences, Nanyang Technological University, 1 Nanyang Walk, Block 5, Level 3, Singapore 637616, Singapore

(Received 29 July 2007; revised manuscript received 3 April 2008; published 19 May 2008)

We present a group theory analysis of the symmetries of the eigenmodes and eigenvalues of photonic crystals with either materially or geometrically anisotropic motif. Irreducible Brillouin zone of such a photonic crystal varies with the parameters of the anisotropic motif. By using coset decomposition of a group, we have identified the irreducible Brillouin zones of such photonic crystals. We have shown the existence of a fundamental zone in the orientations of a motif for which the eigenvalues are found to be unique, and such a zone is fully described by a set of symmetry elements, which form a new group. In addition, by using a two-dimensional photonic crystal with hexagonal lattice as an example, we present a full description of the eigenmode symmetry in the photonic crystal with an anisotropic motif. A classification of degenerate states, which is in the absence of a spatial modulation and in the absence of an anisotropy, is shown by using a properly derived integer system, and the eigenstate splitting (and evolution) in the presence of the anisotropy and the spatial modulation are described in detail.

DOI: 10.1103/PhysRevB.77.195117 PACS number(s): 42.70.Qs, 42.70.Df

I. INTRODUCTION

Photonic crystals (PCs) is an artificial material, which exhibits periodicity either in permittivity or in permeability. Such periodicity resembles that of the electrical potential in a semiconductor and hence enables a PC to control the propagation of photons[1,2] in a similar fashion to electrons being controlled in semiconductors. The ability of PCs to provide a photonic band gap[3] and the extraordinary dispersion relations[4] lead to the invention of novel photonic devices, such as ultrasmall lasers[5] and flat lenses.[6,7]

A PC may be simply viewed as a lattice with a motif attached to each lattice point. The term motif refers to the distribution of the dielectric material within the unit cell of the lattice. If the reorientation of the motif causes the symmetry elements of a PC to change, then the corresponding PC can be defined as an anisotropic PC, as opposed to an isotropic ones. Anisotropic PCs can be geometrically or materially anisotropic. Figure 1 (left) shows the geometry of a two-dimensional (2D) hexagonal lattice PC with a square motif. The orientation of the square motif with respect to the underlying lattice plays a crucial role in determining the optical properties of the 2D PC. In Fig. 1 (right), instead of a square motif, we have a circular motif for which the corresponding orientation is irrelevant. If all materials are isotropic, then the geometry in Fig. 1 represents an example of a geometrically anisotropic and isotropic PCs, respectively. In the presence of an anisotropic material, the optical properties of a PC will vary in accordance to the orientation of the anisotropic material (i.e., the orientation of the principal axes with respect to the lattice), and therefore, the corresponding PC is defined as a materially anisotropic PC. A PC with a geometry in Fig. 1 (right) constitutes an example to the materially anisotropic PC, if either the matrix or the circular cylinders are made of an anisotropic medium. On the other hand, in the presence of an anisotropic material, a PC with a geometry, as shown in Fig. 1 (left), has a mixed anisotropy (i.e., both geometrical and material's anisotropy exist).

Anisotropic PCs have fundamental importance as it is the general class in which isotropic PCs can be considered as a special case. Moreover, anisotropic PCs have been widely used in the design and the applications of PCs. Geometrically, anisotropic PCs have been widely used in exploration of 2D and three-dimensional (3D) photonic band gaps.[8–16] Particularly, in 2D PCs that play a central role in the realization of integrated optical chips, motifs with various geometry have been used to improve the photonic band gap.[8–13] On the other hand, materially anisotropic PCs, apart from their ability to engineer the band gap,[17–20] are found to be extremely useful in realizing tunable PCs.[21–31] Liquid crystal infiltrated 3D[21–24] and 2D[25–30] PCs and PCs with Pockel or Kerr materials[31] are examples of materially anisotropic PCs.

Although anisotropic PCs occur naturally in the design of PCs, adequate theoretical tools based on their symmetry are still lacking. Formal tools for such an analysis can be developed by using group theory, which has been proven to be highly valuable especially in understanding the symmetrical properties of an electronic energy band.[32,33] In the context of a PC, group theory has been employed to investigate mode couplings,[34–37] existence of photonic band gaps,[38] descrip-

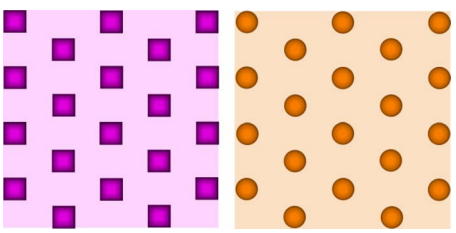

FIG. 1. (Color online) Examples of geometries of a 2D hexagonal lattice PC: square motif (left) and circular motif (right).

 ©2008 The American Physical Society

tion of resonant modes in the defect state of a PC,[39] the symmetrical properties of the eigenmodes of an opal[40] and a metallic photonic crystal,[41] and very recently in the understanding of cutoff conditions of optical vortices in a 2D PC.[42]

In this paper, we develop necessary theoretical tools by using group theory for symmetry analysis of the eigenstates in anisotropic PCs. A systematic description of the irreducible Brillouin zone (IBZ) of an anisotropic PC is given. By using coset decomposition of a group, we have drawn a relationship between the IBZs of isotropic and anisotropic PCs of the same lattice. Moreover, we have elaborated on the existence of a fundamental zone in the orientations of the motif with respect to the lattice. By taking 2D hexagonal lattice as an example, we first introduce an eigenstate classification scheme of degenerate states in the absence of a spatial modulation and in the absence of anisotropy by using a properly derived integer system. We then describe the splitting and the evolution of these states in the presence of the anisotropy and the spatial modulation. The rest of the paper is organized as follows: In Sec. II, we introduce relevant symmetry groups and cosets of an anisotropic PC. In Sec. III, we describe the use of cosets in identifying the IBZs of an anisotropic PC and outline the derivation of the orientational group that leads to the fundamental zone of orientations. In Sec. IV, we give the classification and the evolution of symmetry in an anisotropic 2D PC with an hexagonal lattice. Section V summarizes the key results of the paper and discusses the applicability of the results in the design of anisotropic PCs. Finally, Sec. VI concludes the paper.

II. SYMMETRY GROUPS

The symmetry of a PC is analyzed in terms of their symmetry elements. A collection of symmetry elements that satisfies the group axioms[43,44] is called a symmetry group. Throughout the paper, we denote a symmetry element of a group by using a capital letter Q, the corresponding symmetry group by using the same capital letter but with a bar on top $\bar{Q}$, and the order of the group by using a small version of the same letter q.

A PC is comprised of a lattice and a motif attached to each lattice point. The symmetry operations that leaves the lattice invariant is given by a space group $\bar{G}$. This group have a translational subgroup $\bar{T}$, which contains all primitive translations of the lattice. As $\bar{T}$ is an Abelian group, it has only one-dimensional (1D) irreducible representations (IRs) with the corresponding basis functions,[43,44] which are Bloch functions of a wave vector $\mathbf{k}$. Hence, a magnetic field distribution in a PC constitutes an example for a basis of $\bar{T}$. An action of $T \in \bar{T}$ on the magnetic field function, $\mathbf{H_k}(\mathbf{r})$, can be illustrated as follows:

$$T\mathbf{H_k}(\mathbf{r}) = e^{j\mathbf{kt}}\mathbf{H_k}(\mathbf{r}), \tag{1}$$

where $\mathbf{t}$ is a primitive real lattice vector and $e^{j\mathbf{kt}}$ is an IR of T, which is identified with the wave vector $\mathbf{k}$. Besides the translational symmetry, the lattice comes along with several compatible point group symmetries. The point group of a lattice can be denoted as $\bar{R}$, and the action of R on T ($T \in \bar{T}$ and $R \in \bar{R}$) leaves $\bar{T}$ invariant. Moreover, when R operates on a Bloch function of a wave vector $\mathbf{k}$, it produces another Bloch function with a wave vector $R\mathbf{k}$,[40,43,44]

$$R\mathbf{H_k}(\mathbf{r}) = \mathbf{H'_{Rk}}(\mathbf{r}). \tag{2}$$

Assuming $\bar{G}$ is a symmorphic space group,[43,44] any element of $\bar{G}$ can be expressed as a product of an element of $\bar{T}$ with an element of $\bar{R}$. That is, $\bar{G}=\bar{T}\otimes\bar{R}$, where the sign $\otimes$ indicates the multiplication direction is from the left to right (i.e., semidirect product).[43,44] In a symmorphic space group, all symmetry operations consist of point group operations (i.e., rotations, reflections, and inversions) and translations by using lattice vectors (i.e., belongs to $\bar{T}$) only. Nonsymmorphic space group is more complicated, involving translations by using fractional lattice vectors (not in the group of $\bar{T}$), such as glide reflections and screw rotations; thus, the element of a nonsymmorphic space group cannot be expressed as a product of an element of $\bar{T}$ with an element of the point group. In this paper, all discussions are limited to symmorphic space groups.

Generally, depending on the geometry of the motif and the materials symmetry, the symmetry elements of a motif are different from those of a lattice. The symmetry elements of the motif can be taken as $\bar{R}_{geo}\cap\bar{R}_{mat}$, where $\bar{R}_{geo}$ and $\bar{R}_{mat}$ is, respectively, the geometrical and material point group of the motif. The intersection of two groups is always a group. Thus, the symmetry elements of the motif is also given by a point group, $\bar{R}_B=\bar{R}_{geo}\cap\bar{R}_{mat}$. If the material is isotropic, then $\bar{R}_B=\bar{R}_{geo}$.

Furthermore, an important group in determining the optical properties of a PC is the group of symmetry operations $\bar{G}_M$. The definition of $\bar{G}_M$ can be understood from the following wave equation, which solves the dispersion relation in the PC:

$$M\mathbf{H_k}(\mathbf{r}) = \lambda(\mathbf{k})\mathbf{H_k}(\mathbf{r}), \tag{3}$$

where $\lambda(\mathbf{k})$ is the eigenvalue of a differential operator M.[37,45] The group $\bar{G}_M$ is a subgroup of $\bar{G}$ and contains the symmetry operations G_M, such that

$$G_M M G_M^{-1} = M. \tag{4}$$

Again assuming a symmorphic space group, $\bar{G}_M$ can be expressed as $\bar{G}_M=\bar{T}\otimes\bar{R}_M$, where $\bar{R}_M$ is a point group of M. 2D PCs with symmorphic and nonsymmorphic $\bar{G}_M$ were theoretically previously discussed,[46] and holographic method was proposed for the fabrication.[47] The point group $\bar{R}_M$ is given by

$$\bar{R}_M = \bar{R}\cap\bar{R}_B = \bar{R}\cap\bar{R}_{geo}\cap\bar{R}_{mat}. \tag{5a}$$

If the materials are assumed to be isotropic, then Eq. (5a) becomes

$$\bar{R}_M = \bar{R}\cap\bar{R}_B = \bar{R}\cap\bar{R}_{geo}. \tag{5b}$$

In 2D PC analyses, the wave vectors of light are confined in the 2D periodic plane,[8–13,17,18,25–31] and therefore, the group

TABLE I. $\overline{R_M}$ for typical motifs in a 2D hexagonal lattice. Any two principal axes of the anisotropic material are assumed to be oriented in the 2D periodic plane. Key: sm—geometrical orientation of the motif (or orientation of the principal axes of the anisotropic media) is symmetrically matched with the lattice and arb—arbitrary orientation with no symmetry matching.

		Materials		
			Anisotropic	
Geometry ($\overline{R_{geom}}$)	Orientation	Isotropic	sm	arb
Circle (C_{6v})		C_{6v}	C_{2v}	C_2
Square (C_{4v})	sm	C_{2v}	C_{2v}	C_2
	arb	C_2	C_2	C_2
Rectangle/Ellipse (C_{2v})	sm	C_{2v}	C_{2v}	C_2
	arb	C_2	C_2	C_2
Triangle (C_{3v})	sm	C_{3v}	C_{1h}	C_1
	arb	C_3	C_1	C_1
Hexagon (C_{6v})	sm	C_{6v}	C_{2v}	C_2
	arb	C_6	C_2	C_2

$\overline{R_M}$ is expressed by a plane point group.[34,37,46,47] Table I shows some examples of $\overline{R_M}$ for various motifs in an 2D hexagonal lattice PC ($\bar{R}=C_{6v}$) and the corresponding definition of symmetry elements in the symmetry group can be found in Table X.

In a 3D PC, the definition of M takes the most general form, $M=\nabla\times[1/\tilde{\varepsilon}(\mathbf{r})]\nabla$,[37,45] with $\tilde{\varepsilon}(\mathbf{r})$ as the position-dependent dielectric tensor and Eq. (3) as basically a set of three coupled differential equations. For a 2D PC, there is a possibility of decoupling these coupled equations into two independent equations for the two polarizations of light, namely, H (electric field parallel to the 2D periodic plane) and E (electric field perpendicular to the 2D periodic plane) polarizations. Each of these polarizations satisfies Eq. (3) with a different and independent M.[34,45] It is worth mentioning that if the 2D PC is made of isotropic materials (i.e., only geometrically anisotropic), then we can decouple the two polarizations of light and the corresponding M operators will have the same symmetry groups, $\bar{R}_M$ and $\overline{G_M}$.[34,37] On the other hand, if the 2D PC is made of an anisotropic material (i.e., uniaxial or biaxial) then, in general, the polarizations are coupled. However, a great simplification exists when one of the principal axes of the anisotropic material is perpendicular to the 2D periodic plane, where we can decouple the polarizations into E and H polarizations.[17,18,25,27,28] In this case, the two M operators for the two polarizations may have different $\overline{G_M}$. The electric field in the E polarization is parallel to the principal axis that is lying perpendicular to the 2D periodic plane, the symmetry of the E polarization is therefore not affected by the anisotropy of the material, and consequently, the corresponding $\overline{G_M}$ is the same as if the 2D PC is constructed with isotropic materials [i.e., $\bar{R}_M$ is given by Eq. (5b)], whereas for the H polarization, the $\overline{G_M}$ is obviously influenced by the material symmetry [i.e., $\bar{R}_M$ is given by Eq. (5a)].[18,25,27]

A subgroup of groups $\bar{G}$, $\bar{R}$, $\overline{G_M}$, and $\overline{R_M}$ can be formed for each wave vector $\mathbf{k}$ by considering the corresponding symmetries in $\mathbf{k}$. From Eq. (1), each 1D IR of $\bar{T}$ is given by $e^{j\mathbf{k}t}$. Since, $e^{j\mathbf{G}t}=1$ (where $\mathbf{G}$ is the reciprocal lattice vector), two IRs of $\bar{T}$ identified by wave vectors, $\mathbf{k}$ and $\mathbf{k}+\mathbf{G}$, are essentially the same. Thus, the elements of $\bar{G}$, whose action on $\mathbf{k}$ generates $\mathbf{k}$ added with multiples of $\mathbf{G}$, form a subgroup, $\bar{G}(\mathbf{k})$. Similarly, we can form subgroups $\bar{R}(\mathbf{k})$, $\overline{G_M}(\mathbf{k})$, and $\overline{R_M}(\mathbf{k})$ from the main groups of $\bar{R}$, $\overline{G_M}$, and $\overline{R_M}$, respectively, by considering the symmetries in $\mathbf{k}$. Figure 2 depicts the relationships among the groups $\bar{R}$, $\overline{R_B}$, $\overline{R_M}$, $\bar{R}(\mathbf{k})$, and $\overline{R_M}(\mathbf{k})$. Any symmorphic space group can be written as a product of $\bar{T}$ and a point group. For groups of $\mathbf{k}$, this product is a direct product (i.e., the multiplication direction is irrelevant). For instance, $\bar{G}=\bar{T}\otimes\bar{R}$ is a semidirect product, but $\bar{G}(\mathbf{k})=\bar{T}\times\bar{R}(\mathbf{k})$ is a direct product.[43,44]

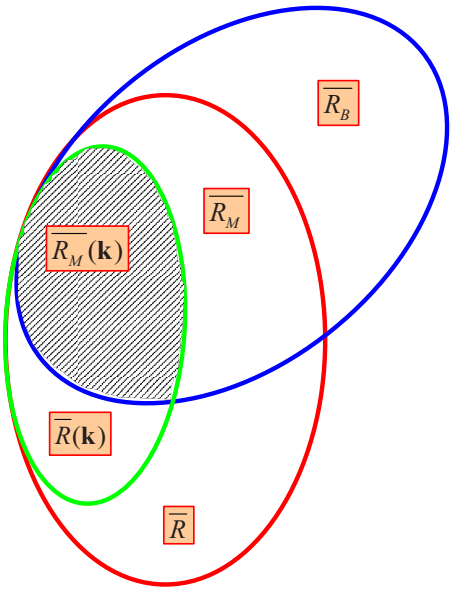

FIG. 2. (Color online) Set relationships between $\bar{R}$, $\overline{R_B}$, $\overline{R_M}$, $\bar{R}(\mathbf{k})$, and $\overline{R_M}(\mathbf{k})$.

In discussing the properties of a group, a useful tool is a coset decomposition.[43,44] When an element of a group acts on its subgroup, it produces a set of elements called coset. A group may have several (an integer number) distinct cosets depending on the size of the subgroup. Based on the group properties, all cosets of a group (derived from the same subgroup) must be the same in size and must be either identical or totally different sets (i.e., no elements in common between any two cosets). Hence, a group can be decomposed into a sum of distinct cosets. For instance, a coset decomposition that will be useful in the later discussion,

$$\overline{G_M}=\overline{G_M}(\mathbf{k})G_{M1}+\overline{G_M}(\mathbf{k})G_{M2}+\cdots+\overline{G_M}(\mathbf{k})G_{M[r_m/r_m(k)]}. \tag{6a}$$

In the above coset decomposition, $G_{Mi}\in\overline{G_M}[i=1,2,\ldots,r_m/r_m(\mathbf{k})]$, and $\overline{G_M}$ is decomposed with respect to its subgroup, $\overline{G_M}(\mathbf{k})$. $\overline{G_M}(\mathbf{k})G_{Mi}$ is said to be a "right coset" as the action of G_{Mi} is on the right to $\overline{G_M}(\mathbf{k})$. The number of cosets is given by the ratio of the orders of the group and the

subgroup, $g_m/g_m(\mathbf{k})$, and it has to be an integer. Since $\overline{G_M}$ and $\overline{G_M}(\mathbf{k})$ is a product of $\bar{T}$ with $\overline{R_M}$ and $\overline{R_M}(\mathbf{k})$, respectively, $g_m/t=r_m/r_m(\mathbf{k})$. In addition, as the factor group $\overline{G_M}/\bar{T}$ is isomorphic to R_M, Eq. (6a) can be equivalently written as

$$\overline{R_M} = R_{M1} + R_{M2} + \cdots + R_{M[r_m/r_m(k)]}, \tag{6b}$$

where R_{Mi} is taken from each coset of $\overline{R_M}$ decomposed with respect to $\overline{R_M}(\mathbf{k})$. An important property of a coset is that if $\varphi(\mathbf{r})$ is a basis for an IR of a subgroup, the function $Q\varphi(\mathbf{r})$ is a basis for a representation of the main group $\bar{Q}$, provided Q is chosen from a coset of $\bar{Q}$ expanded with respect to the same subgroup.

The coset decomposition of a group will be used in Sec. III A. Specifically, the coset decomposition of $\overline{G_M}$ with respect to $\overline{G_M}(\mathbf{k})$ will be used in the description of the IBZ of an anisotropic PC, and the coset decomposition of $\bar{R}$ with respect to $\overline{R_M}$ will be used to relate the IBZ of the isotropic and the IBZ of the anisotropic PC of the same lattice.

III. SYMMETRY IN THE WAVE EQUATION

A. Irreducible Brillouin zones

In this section, we shall present the IBZ formulation of an anisotropic PC and the relationship between this IBZ and the IBZ of an isotropic PC of the same lattice. The IBZ of an isotropic PC is fixed once the lattice is known; therefore, it can also be called as IBZ of the lattice. Although the IBZ of an anisotropic PC has previously been inferred for some simple and specific 2D structures,[8,18] the present paper is the first systematic and general study of IBZ for anisotropic PCs by using group theory. The formalism in this section will provide a systematic set of tools in describing IBZ of anisotropic PC and therefore enables to predict IBZ of a more complex 2D and 3D PC structures.

Consider the symmetry operations that leaves M invariant in Eq. (3) at a particular $\mathbf{k}$ vector. Such a symmetry operations comes from $\overline{G_M}(\mathbf{k})$. Operate $G_M(\mathbf{k})$, $G_M(\mathbf{k}) \in \overline{G_M}(\mathbf{k})$ on both sides of Eq. (3), and as M commutes with $G_M(\mathbf{k})$ [Eq. (4)],

$$M[G_M(\mathbf{k})\mathbf{H}_\mathbf{k}(\mathbf{r})] = \lambda(\mathbf{k})[G_M(\mathbf{k})\mathbf{H}_\mathbf{k}(\mathbf{r})]. \tag{7}$$

Equation (7) shows that $G_M(\mathbf{k})\mathbf{H}_\mathbf{k}(\mathbf{r})$ is an eigenfunction of M. By using group representation, we can write $G_M(\mathbf{k})\mathbf{H}_\mathbf{k}(\mathbf{r})$ as a sum of basis functions of an IR of $\overline{G_M}(\mathbf{k})$,

$$G_M(\mathbf{k})\mathbf{H}_\mathbf{k}(\mathbf{r}) = \sum_{j=1}^{d} a_j \mathbf{H}_\mathbf{k}^j(\mathbf{r}), \tag{8}$$

where $G_M(\mathbf{k}) \in \overline{G_M}(\mathbf{k})$, $\mathbf{H}_\mathbf{k}^j(\mathbf{r})$, with $j=1,\ldots,d$, is a basis function of a d-dimensional IR of $\overline{G_M}(\mathbf{k})$, and a_j is a scalar coefficient.

A complete set of symmetry operations that leaves M invariant is given by the space group $\overline{G_M}$. From Eqs. (3) and (4), for any $G_M \in \overline{G_M}$,

$$M[G_M\mathbf{H}_\mathbf{k}(\mathbf{r})] = \lambda(\mathbf{k})[G_M\mathbf{H}_\mathbf{k}(\mathbf{r})]. \tag{9}$$

Clearly $G_M\mathbf{H}_\mathbf{k}(\mathbf{r})$ is an eigenfunction of M. Hence, as we did for $G_M(\mathbf{k})\mathbf{H}_\mathbf{k}(\mathbf{r})$ [Eq. (8)], $G_M\mathbf{H}_\mathbf{k}(\mathbf{r})$ can be written as a linear combination of basis functions of an IR of $\overline{G_M}$. The basis function of its subgroup, $\overline{G_M}(\mathbf{k})$, is given by $\mathbf{H}_\mathbf{k}^j(\mathbf{r})$, where $j=1,\ldots,d$ [Eq. (8)]; thus, from the coset decomposition [Eqs. (6a) and (6b)], we know that $R_{Mi}\mathbf{H}_\mathbf{k}^j(\mathbf{r})$, where $i=1,\ldots,s=r_M/r_M(\mathbf{k})$, with R_{Mi} belonging to each coset of $\overline{R_M}$ decomposed with respect to $\overline{R_M}(\mathbf{k})$, must be a basis function of a representation of $\overline{G_M}$. In this particular case it can be shown that this representation is also irreducible (see pp. 124 and 125 of Ref. 43). By using Eq. (2), the basis function of an IR of $\overline{G_M}$, $R_{Mi}\mathbf{H}_\mathbf{k}^j(\mathbf{r})$, can be written as $\mathbf{H}_{R_{Mi}\mathbf{k}}^j(\mathbf{r})$. Therefore, the eigenfunction of M, $G_M\mathbf{H}_\mathbf{k}(\mathbf{r})$ [Eq. (9)], can be written as a linear combination of sd-independent basis functions of an IR of $\overline{G_M}$, as follows:

$$G_M\mathbf{H}_\mathbf{k}(\mathbf{r}) = \sum_{i=1}^{s}\sum_{j=1}^{d} b_{i,j}\mathbf{H}_{R_{Mi}\mathbf{k}}^j(\mathbf{r}), \tag{10}$$

where $b_{i,j}$ is a scalar coefficient. Equation (10) shows that the eigenspace of Eq. (3), with an eigenvalue of $\lambda(\mathbf{k})$, is spanned by sd number of independent basis functions, $\mathbf{H}_{R_{Mi}\mathbf{k}}^j(\mathbf{r})$ (i.e., sd-fold degeneracy).

For a general wave vector, $\overline{R_M}(\mathbf{k})$ contains only the identity element and so only one 1D IR (i.e., $d=1$) and $s=r_M$. Thus, the eigenvalue for a general wave vector is r_M-fold degenerate with r_M basis functions formed by r_M-$\mathbf{k}$ vectors in the first BZ. However, it is sufficient to use only one of these vectors to obtain the eigenvalue. So, among the zone of vectors defined in the first BZ, only $1/r_M$ portion of wave vectors will have nondegenerate eigenvalue. That $1/r_M$ portion is the irreducible part of the BZ (IBZ) of the anisotropic PC. For example, we illustrate the IBZs for a 2D hexagonal lattice PC in Fig. 3 for various $\overline{R_M}$. In Fig. 3(a), we have $\overline{R_M}=\bar{R}=C_{6v}$, so $r_M=12$ and the $1/r_M$ portion of the hexagonal BZ is a triangle, as shown in the figure. Figures 3(b)–3(f) show the IBZs for $\overline{R_M}=C_{3v}$, C_{2v},C_2, C_1, and $C_{2v'}$, respectively. The definition of the first four groups can be found in the Table X. The group $C_{2v'}$ is similar to C_{2v}; however, the two mirror axis are σ_{-30° and σ_{60°, respectively.

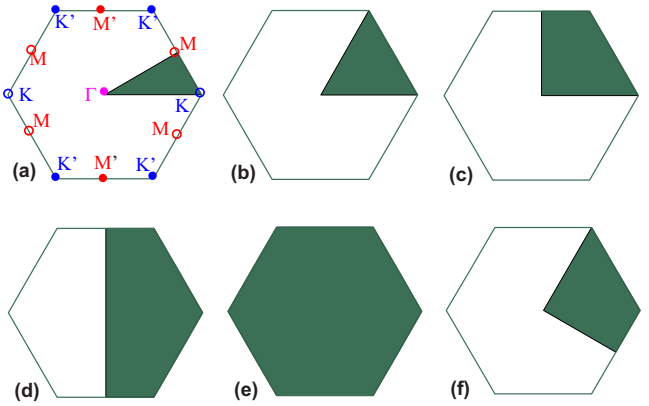

FIG. 3. (Color online) IBZs when $\overline{R_M}(\mathbf{k})$ equals to (a) C_{6v}, (b) C_{3v}, (c) C_{2v}, (d) C_2, (e) C_1, and (f) $C_{2v'}$. Symmetrical points of a 2D hexagonal lattice are labeled in (a).

As we described in Sec. I, apart from the symmetry of the lattice, the definition of $\overline{G_M}$ is determined by the materials

and the geometry of the motif. So, the definition of the IBZ and the optical properties will vary when the elements of $\overline{G_M}$ varies. On the other hand, it is always possible to define an IBZ, which is reduced from the BZ by using the symmetries of the lattice $\bar{G}$. Such an IBZ is that of the PC when $\overline{G_M}=\bar{G}$ and can be named as IBZ of the lattice (the IBZ of the lattice refers to that of an isotropic PC of the same lattice). Given a lattice, $\bar{G}$ is fixed; however, there could be many possibilities of its subgroup $\overline{G_M}$. Thus, it is useful to draw a relationship between $\bar{G}$ and $\overline{G_M}$ so that the optical properties that belongs to $\overline{G_M}$ can be obtained by means of $\bar{G}$. Such a relationship can be found using a coset decomposition of $\bar{G}$ with respect to its subgroup $\overline{G_M}$,

$$\bar{G}=\overline{G_M}G_1+\overline{G_M}G_2+\cdots+\overline{G_M}G_{g/g_m}, \tag{11}$$

where $G_i\in\bar{G}$ and there are g/g_m distinct cosets. Since $\bar{G}=\bar{T}\otimes\bar{R}$, factor group $\bar{G}/\bar{T}$ is isomorphic to $\bar{R}$. Thus, $g/g_m=r/r_m$ and for $R_i\in\bar{R}$, equivalently, Eq. (11) can be written as

$$\bar{R}=\overline{R_M}R_1+\overline{R_M}R_2+\ \ldots\ +\overline{R_M}R_{r/r_m}. \tag{12}$$

Any R_j of the same coset $\overline{R_M}R_i$ can be written as $R_j=R_{Mj}R_i$, where $R_{Mj}\in\overline{R_M}$, without changing the coset representative R_i. Since ${R_{Mj}}^{-1}MR_{Mj}=M$, an operator defined as $R^{-1}MR$ remains unchanged for R belonging to the same coset. If R belongs to different cosets, $R^{-1}MR$ is essentially different. Hence, there are r/r_m different $R^{-1}MR$ operators with R chosen from each coset, $\overline{R_M}R_i$.

For a wave vector $R\mathbf{k}$ with $R\in\bar{R}$, the corresponding eigenvalue is denoted as $\lambda(R\mathbf{k})$. From Eq. (3), we have

$$M\mathbf{H}_{R\mathbf{k}}(\mathbf{r})=\lambda(R\mathbf{k})\mathbf{H}_{R\mathbf{k}}(\mathbf{r}). \tag{13}$$

Since $\mathbf{H}_{R\mathbf{k}}(\mathbf{r})=R\mathbf{P}_{\mathbf{k}}(\mathbf{r})$ with $\mathbf{P}_{\mathbf{k}}(\mathbf{r})$ being another Bloch function [Eq. (2)], Eq. (13) can be rearranged for any R ($R\in\bar{R}$),

$$R^{-1}MR[\mathbf{P}_{\mathbf{k}}(\mathbf{r})]=\lambda(R\mathbf{k})[\mathbf{P}_{\mathbf{k}}(\mathbf{r})]. \tag{14}$$

With the absence of the anisotropic motif (i.e., isotropic PC with $\overline{R_M}=\bar{R}$), $R^{-1}MR=M$ for all R. Hence, $\lambda(R\mathbf{k})=\lambda(\mathbf{k})$ for all R, $R\in\bar{R}$. However, with the presence of anisotropic motif, there will be r/r_M different eigenvalues since there are r/r_M distinct $R^{-1}MR$ operators. This also means that among r wave vectors $R\mathbf{k}$ that are equivalent with the absence of the anisotropic motif will split into r/r_M sets of in-equivalent $R\mathbf{k}$ wave vectors. Thus, the size of PC's IBZ is enlarged by a factor of r/r_M compared to the size of the IBZ of the latttice. From the coset decomposition, we know that r/r_M must be an integer and this means the size of PC's IBZ is an integer multiples of size of the IBZ of the lattice. Furthermore, if the IBZ of the lattice is denoted as a collection of wave vectors $[\mathbf{k}]$, then the IBZ of the anisotropic PC is a collection of $R_1[\mathbf{k}],\ldots,R_{r/r_M}[\mathbf{k}]$, with R_i chosen from each coset in Eq. (12).

This result is very useful in identifying the IBZs of complicated 3D anisotropic PCs and a quick verification can be illustrated by using Fig. 3 for various $\overline{R_M}$ when $\bar{R}=C_{6v}$. For instance, when $\overline{R_M}=C_{2v}$, the IBZ of the PC is $r/r_M=3$ times bigger than the IBZ of the lattice. The IBZ of the lattice is a zone of wave vectors $[\mathbf{k}]$ shown in a triangle of Fig. 3(a). If $C_{2v}=[E\ C_2\ \sigma_0\ \sigma_{90^\circ}]$ (Table X), the coset decomposition $\bar{R}=C_{6v}$ with respect to $\overline{R_M}=C_{2v}$ takes the form of $\bar{R}=C_{2v}E+C_{2v}R_2+C_{2v}R_3$, where R_2 and R_3 are the coset representatives. Hence, the IBZ of the PC with $\overline{R_M}=C_{2v}$ is given by a collection of wave vectors, $E[\mathbf{k}]$, $\sigma_{30^\circ}[\mathbf{k}]$, and $C_6[\mathbf{k}]$, where E, σ_{30°, and C_6 are chosen from each coset of C_{2v} ($\overline{R_M}$) with respect C_{6v} ($\bar{R}$). Such a collection of wave vectors forms the shaded region in Fig. 3(c). It has to be noted that the definition of an IBZ depends on the explicit definition of $\overline{R_M}$. For example, if $C_{2v}=[E\ C_2\ \sigma_{-30^\circ}\ \sigma_{60^\circ}]$ (i.e., $C_{2v'}$), the definition of cosets changes and this implies a change in IBZ, as shown in Fig. 3(f).

As we have shown, the definition of IBZ of an anisotropic PC changes with the definition of $\overline{R_M}$, although the lattice group $\bar{R}$ does not change. The IBZ of the anisotropic PC can be obtained by transforming the wave vectors $\mathbf{k}$ in the IBZ of the lattice by using the operations $R\mathbf{k}$, where R is selected from each coset of $\bar{R}$ expanded with respect to $\overline{R_M}$. Therefore, in PCs (2D or 3D) with anisotropic materials, if the optical properties (i.e., band gaps) are to be monitored as a function of optic axis, the varying optic axis will change $\overline{R_M}$ and demands redefinition of IBZ for each orientation of optic axis. This may not be desired as redefinition of IBZ requires the knowledge of cosets for each orientation of optic axis. An alternative way to such a redefinition can be obtained by using Eq. (14). Eigenvalue with a wave vector $R\mathbf{k}$, $\lambda(R\mathbf{k})$, can be obtained from a wave vector $\mathbf{k}$, but with a coordinate transformed M operator, $R^{-1}MR$. By selecting R from each coset of $\bar{R}$ expanded with respect to $\overline{R_M}$, we can find the eigenvalues at all inequivalent $R\mathbf{k}$ vectors from a single $\mathbf{k}$ vector. Thus, regardless of $\overline{R_M}$, we can fix the IBZ as that of the lattice; however, the computations has to be repeated r/r_m times with distinct $R^{-1}MR$ operators. This method is advantageous as it may not require the knowledge of group theory (cosets) in the numerical implementation. A simple coding can accomplish the task to find all (r/r_m in total) distinct $R^{-1}MR$ operators. The evaluation of $R^{-1}MR$ is straightforward from the fact $R^{-1}MR=R^{-1}M[\tilde{\varepsilon}(\mathbf{r})]R=M[R^{-1}\tilde{\varepsilon}(\mathbf{r})R]$, where $M[\tilde{\varepsilon}(\mathbf{r})]$ and $M[R^{-1}\tilde{\varepsilon}(\mathbf{r})R]$ represent M as a function of $\tilde{\varepsilon}(\mathbf{r})$ and $R^{-1}\tilde{\varepsilon}(\mathbf{r})R$, respectively (see Ref. 37 for a proof). The task gets further simplified if the problems involves materially anisotropic PCs with only one isotropic material,[17–31] where $R^{-1}\tilde{\varepsilon}(\mathbf{r})R$ becomes $R^{-1}\tilde{\varepsilon}_aR$, where $\tilde{\varepsilon}_a$ is the dielectric tensor of the anisotropic material.

B. Fundamental zone of orientations

The reorientation of the motif with respect to the lattice will change the symmetry elements of $\overline{R_M}$. In this section, we analyze the consequence of such symmetry variation as a function of an orientational parameter. The orientational parameter θ can be defined by using the angle between two symmetry axes of $\bar{R}$ and $\overline{R_M}$, respectively. As $\overline{R_M}$ is dependent on θ (Table I), it will be useful to denote $\overline{R_M}$ as $\overline{R_M}(\theta)$. When the orientation of the motif is parallel to the symmetri-

cal directions of the lattice, $\overline{R_M}(\theta)$ is obviously a larger group than $\overline{R_M}(\theta)$ of a general orientation for which none of the symmetrical axis overlaps (Table I). Moreover, for a general orientation, $\overline{R_M}(\theta)$ is an invariant subgroup of $\bar{R}$ (or a normal subgroup[43,44]). For instance, in a 2D PC, the symmetrical axes are mirror axes (in the periodic plane), and for a general orientation, the entire elements in the class[43,44] containing mirror elements are removed. If rotations exist in $\overline{R_M}(\theta)$, they should exist as a whole class and obviously are not disturbed by any orientation of the motif in the periodic plane as the rotational axis is perpendicular to the 2D periodic plane. For instance, considering an hexagonal lattice, $\bar{R}=C_{6v}$, a motif with $\overline{R_B}=C_{2v}$ and defining the angle between the σ_0 axis in $\bar{R}$ and the σ_0 axis in $\overline{R_B}$ to be θ, when θ equals to the multiples of 30° (i.e., orientation of the motif matches symmetrical directions of hexagonal lattice) $\overline{R_M}(\theta)=C_{2v}$, and for all any other angle, we have a smaller group of $\overline{R_M}(\theta)=C_2$ (Table I). Thus, for the general orientation, $R_M(\theta)=C_2$, which is obviously an invariant subgroup of $\bar{R}=C_{6v}$.

Assuming that when $\theta=\alpha$, $M=M_\alpha$ with an eigenvalue of $\lambda_\alpha(\mathbf{k})$, Eq. (3) becomes $M_\alpha \mathbf{H}_\mathbf{k}(\mathbf{r})=\lambda_\alpha(\mathbf{k})\mathbf{H}_\mathbf{k}(\mathbf{r})$. The reorientation causes θ to change to a new value, $\theta=\beta$, M_α changes to M_β, $M_\beta=R_\theta^{-1}M_\alpha R_\theta$, and $\lambda_\alpha(\mathbf{k})$ changes to $\lambda_\beta(\mathbf{k})$. Thus, when $\theta=\beta$, the eigenequation becomes

$$R_\theta^{-1}M_\alpha R_\theta[\mathbf{H}_\mathbf{k}(\mathbf{r})]=\lambda_\beta(\mathbf{k})[\mathbf{H}_\mathbf{k}(\mathbf{r})]. \tag{15}$$

If $R_\theta \in \overline{R_M}(\alpha)$, then $R_\theta^{-1}M_\alpha R_\theta=M_\alpha$ and $\lambda_\beta(\mathbf{k})=\lambda_\alpha(\mathbf{k})$. Furthermore, even if $R_\theta \notin \overline{R_M}(\alpha)$, however, $R_\theta \in \bar{R}(\mathbf{k})$, following Eq. (2), we still have $\lambda_\beta(\mathbf{k})=\lambda_\alpha(\mathbf{k})$. In fact, there could be more symmetry elements other than $\overline{R_M}(\alpha)$ and $\bar{R}(\mathbf{k})$. It can be easily shown a set of orientational operations $[R_\theta]$ $R_\theta=R_M R$, where $R_\theta \in [R_\theta]$ [not necessarily belongs to $\overline{R_M}(\alpha)$ or $\bar{R}(\mathbf{k})$], $R_M \in \overline{R_M}(\alpha)$, and $R \in \bar{R}(\mathbf{k})$, for which Eq. (15) is invariant, leading to the same eigenvalue. $[R_\theta]$ is a subset of $\bar{R}$ whose set order can be written as

$$|r_\theta|=\frac{r(\mathbf{k})r_m(\alpha)}{r_m(\mathbf{k})}. \tag{16}$$

It is worth mentioning that $\overline{R_M}(\mathbf{k})=\bar{R}(\mathbf{k})\cap\overline{R_M}(\alpha)$ (Fig. 2) and $\overline{R_M}(\mathbf{k})\subset\bar{R}(\mathbf{k})$ (Fig. 2). In Eq. (16), $|r_\theta|$ is an integer as the division of the orders of the group and the subgroup must be an integer.

The set $[R_\theta]$ does not necessarily form a group, although mostly it does. If $\overline{R_M}(\alpha)$ is a subgroup of $\bar{R}(\mathbf{k})$, then $\overline{R_M}(\mathbf{k})=\overline{R_M}(\alpha)$, $|r_\theta|=r(\mathbf{k})$, and $[R_\theta]=\bar{R}(\mathbf{k})$. Inversely, if $\bar{R}(\mathbf{k})$ is a subgroup of $\overline{R_M}(\alpha)$, then $\overline{R_M}(\mathbf{k})=\bar{R}(\mathbf{k})$, $|r_\theta|=r_m(\alpha)$, and $[R_\theta]=\overline{R_M}(\alpha)$. If either $\bar{R}(\mathbf{k})$ or $\overline{R_M}(\alpha)$ is an invariant subgroup of $\bar{R}$, then it can be easily verified that they form a group with the order given by Eq. (16). Moreover, if $\overline{R_M}(\mathbf{k})=E$, $[R_\theta]$ is a direct product group between $\bar{R}(\mathbf{k})$ and $\overline{R_M}(\alpha)$.

Hence, for a general orientation for which $\overline{R_M}(\alpha)$ is an invariant subgroup of $\bar{R}$, $[R_\theta]$ is a group and can be denoted as a group of orientation R_θ. This group of orientation is fundamentally important because all orientations have minimum symmetry of $\overline{R_\theta}$. The existence of symmetry in the orientations leads to a fundamental zone of orientations (FZO), in which the orientations within the zone have unique eigenvalues. Such a fundamental zone can be obtained by considering the symmetry of $\overline{R_\theta}$. For example, the groups of $\overline{R_\theta}$ for various $\mathbf{k}$ vectors of a 2D hexagonal lattice and $\overline{R_M}$ are listed in Table II. The respective definition of the FZO for $\overline{R_\theta}$ is presented in Table III based on the symmetry elements listed in Table X. Similar to an IBZ definition, the definition of a FZO depends on the explicit definitions of the symmetry elements. For instance, when $\overline{R_\theta}=C_{2v}=[E\ C_2\ \sigma_0\ \sigma_{90°}]$, the FZO is $0<\theta<90°$ (Table III), where else if the mirror elements in C_{2v} change to $\sigma_{-30°}$ and $\sigma_{60°}$ (i.e., $\overline{R_\theta}=C_{2v'}$), then the FZO changes to $-30°<\theta<60°$.

A clearer representation of a FZO can be accomplished by using a diagram. If the orientation of the motif is represented as a unit vector, then the FZO of a 2D PC can be represented in a unit circle. The FZO of a 2D PC with $\overline{R_\theta}=C_{3v}$, C_{2v}, $C_{2v'}$, and C_6 is shown in Figs. 4(a)–4(d), respectively. The shaded region in each circle represents the corresponding FZO. Such a sketch of FZO is advantageous as the symmetry operations of $\overline{R_\theta}$ can be highlighted in the diagram. For example, the thick lines in Fig. 4(a)–4(c) represent the mirror operations in $\overline{R_\theta}$, whereas the centered ellipse, triangle, and hexagon

TABLE II. $\overline{R_\theta}$ at various $\mathbf{k}$ vectors and for various $\overline{R_M}$ of general orientations in a 2D hexagonal lattice. The $\overline{R_\theta}$ groups formed by a direct product between $\bar{R}(\mathbf{k})$ and a $\overline{R_M}$ of a general orientation are underlined.

	$\overline{R_M}$			
$\mathbf{k}$ points (π/a)	C_6	C_3	C_2	C_1
Γ (0,0)	C_{6v}	C_{6v}	C_{6v}	C_{6v}
K $(4/3,0)$	C_{6v}	C_{3v}	$\underline{C_{6v}}$	C_{3v}
M $(1,-1/\sqrt{3})$	C_{6v}	$\underline{C_{6v}}$	C_{2v}	C_{2v}
J (along MK)	$\underline{C_{6v}}$	$\underline{C_{3v}}$	$\underline{C_{2v}}$	C_{1h}
T (along ΓK)	$\underline{C_{6v}}$	$\underline{C_{3v}}$	$\underline{C_{2v}}$	C_{1h}
Σ (along ΓM)	$\underline{C_{6v}}$	$\underline{C_{3v}}$	$\underline{C_{2v}}$	C_{1h}
L (along ΓJ)	C_6	C_3	C_2	C_1

TABLE III. FZO for various $\overline{R_\theta}$ that are compatible with a 2D hexagonal lattice with γ as an arbitrary positive angle. The definitions are based on the symmetry elements of Table X.

$\overline{R_\theta}$	FZO
C_{6v}	$0<\theta<30°$
C_{3v}	$0<\theta<60°$
C_{2v}	$0<\theta<90°$
C_6	$\gamma<\theta<\gamma+60°$
C_3	$\gamma<\theta<\gamma+120°$
C_{1h}	$0<\theta<180°$
C_2	$\gamma<\theta<\gamma+180°$
C_1	$\gamma<\theta<\gamma+360°$

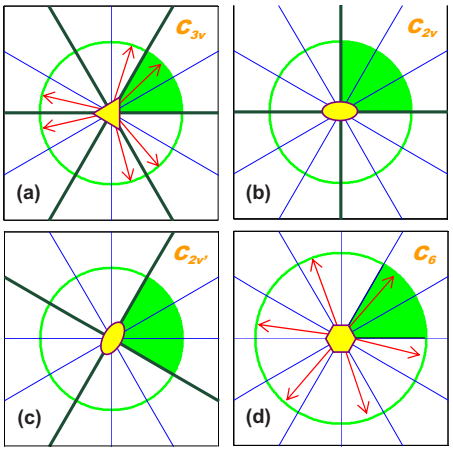

FIG. 4. (Color online) FZO when $\overline{R_\theta}$ equals to (a) C_{3v}, (b) C_{2v}, (c) $C_{2v'}$, and (d) C_6. The thick lines represent the symmetrical axes of $\overline{R_\theta}$, whereas the ellipse, triangle, and hexagon represent the twofold, threefold, and sixfold rotational operations of $\overline{R_\theta}$. The red arrows in (a) and (d) denote the equivalent orientations in each case.

represents the twofold, threefold, and sixfold rotational operations of $\overline{R_\theta}$, respectively. Although C_{3v} and C_6 may have the same FZO [Figs. 4(a) and 4(d)], C_6 does not have any mirror operations and this makes the definition of equivalent orientations in both C_{3v} and C_6 different. The equivalent orientations in each case are shown in Figs. 4(a) and 4(d), respectively.

The concept of FZO is also applicable for 3D anisotropic PCs. All possible orientations of the motif in the 3D space can be represented in an unit sphere. Therefore, the existence of orientational symmetry (given by the group $\overline{R_\theta}$) will reduce the sphere to a 3D FZO, for which the respective orientations produce unique eigenvalues for Eq. (3). The corresponding orientational group for the 3D PC must consist of all symmetry operations, $R_\theta = R_M R$, with $R_M \in \overline{R_M}$ of general orientation of the motif in the 3D space and $R \in \bar{R}(\mathbf{k})$. In 3D anisotropic PCs, instead of the whole 3D space, we could look for fundamental orientations of the motif within a particular plane of choice in the 3D space. In such case, the fundamental orientations of motif in the plane of choice can be obtained by constructing an orientational group consist of symmetry operations $R_\theta = R_M R$ with $R_M \in \overline{R_M}$ of general orientation in the plane of interest and $R \in \bar{R}(\mathbf{k})$. It is worth mentioning that in this case, instead of an unit sphere, we can use an unit circle to represent the FZO of the 3D anisotropic PC in the plane of interest.

On the other hand, the effect of the orientation to an eigenfunction is straightforward. To see this, rearranging Eq. (15) to $M_\alpha[R_\theta \mathbf{H}_\mathbf{k}(\mathbf{r})] = \lambda_\beta(\mathbf{k})[R_\theta \mathbf{H}_\mathbf{k}(\mathbf{r})]$, we can see that when $R_\theta \in \overline{R_\theta}$, but $R_\theta \notin \overline{R_M}(\mathbf{k})$, the eigenfunction at $\theta = \beta$ is a rotated version of the one at $\theta = \alpha$. If $R_\theta \in \overline{R_M}(\mathbf{k})$, the eigenfunctions at $\theta = \beta$ and $\theta = \alpha$ remain unaltered. Applications and examples of FZO appear in Sec. IV B 3.

It is worth mentioning that the definition of IBZ and FZO is dependent on the symmetry of the point group $\overline{R_M}$. As we have mentioned in Sec. II that [see the paragraph after Eq. (5b)] in a 2D materially anisotropic PC, if the polarizations can be decoupled, the operator M generally splits into two independent operators with different $\overline{R_M}$. Therefore, the corresponding IBZ and FZO will be polarization dependent.

IV. SYMMETRY OF THE EIGENMODES

From Eq. (10), we know that the complete set of independent eigenfunctions that span the eigenspace with an eigenvalue λ in Eq. (3) is the basis functions of an IR of $\overline{G_M}$ [i.e., $\mathbf{H}^j_{R_{Mi}\mathbf{k}}(\mathbf{r})$]. Thus, the IR of $\overline{G_M}$ can be used to label and describe the symmetry of the eigenmode. However, it will be useful and easy if we can identify the symmetry of the eigenmode by using a point group representation. Since $\overline{G_M}$ is a semidirect product between $\bar{T}$ and $\overline{R_M}$, the corresponding IR of $\overline{G_M}$ cannot be simply associated with those of $\overline{R_M}$.[43,44]

If we concentrate on a particular $\mathbf{k}$, then the assignment of an IR to the eigenvalue becomes more apparent and simple. Such a representation is called a small representation.[44] From Eq. (8), we know that the complete set of basis functions at a particular $\mathbf{k}$ that gives the same eigenvalue is given by the set of basis functions of an IR of $\overline{G_M}(\mathbf{k})$ [i.e., $\mathbf{H}^j_\mathbf{k}(\mathbf{r})$, with $j = 1, \ldots, d$]. As $\overline{G_M}(\mathbf{k}) = \bar{T} \times \overline{R_M}(\mathbf{k})$ is a direct product, by group theoretical arguments[43] and by using Eq. (1), we have

$$\Gamma[G_M(\mathbf{k})] = \Gamma(T)\Gamma[R_M(\mathbf{k})] = e^{j\mathbf{k}\mathbf{t}}\Gamma[R_M(\mathbf{k})], \qquad (17)$$

where $G_M(\mathbf{k}) \in \overline{G_M}(\mathbf{k})$, $T \in \bar{T}$, $R_M(\mathbf{k}) \in \overline{R_M}(\mathbf{k})$, and $\Gamma(Q)$ denotes a representation of a symmetry element Q. The dimension of $\Gamma(T)$ is one (Sec. II), thus the dimension of $\Gamma[G_M(\mathbf{k})]$ is determined by the dimension of $\Gamma[R_M(\mathbf{k})]$. The eigenmode symmetry then can be identified with an IR of $\overline{R_M}(\mathbf{k})$, which is a point group and the corresponding IRs can be readily obtained from the standard literatures of crystallographic group theory.[43,44] The IRs of the group C_{6v} and the IRs of the compatible subgroups are listed in Table X.

Degeneracy of a state is determined by the dimension of the IR of $\overline{R_M}(\mathbf{k})$, d, that labels the eigenvalue. This can be seen from Eqs. (8) and (17), where at a particular $\mathbf{k}$ vector, the eigenspace is spanned by d-number basis functions. Therefore, the degeneracy of the state with a d-dimensional IR of $\overline{R_M}(\mathbf{k})$ must be d. However, there could be additional degeneracy resulted from the crossing of bands or the absence of spatial modulation. Such a degeneracy, which cannot be explained by using the IR dimension, is termed as an accidental degeneracy.[43,44] A systematical method to determine accidental degeneracy in the absence of spatial modulation will be shown in Sec. IV A for the symmetrical $\mathbf{k}$ vectors of the hexagonal lattice.

In order to illustrate the symmetry of the eigenmodes and the eigenvalues in a PC, we use an example of a 2D PC with an hexagonal lattice and circular cylinders with a radius to period ratio of r_c. We assume the cylinders to be isotropic with a refractive index of 3.5 (silicon) and the matrix medium to be uniaxially anisotropic with an ordinary refractive index n of 1.6 and a birefringence of Δn. Such a uniaxial medium can be a wide range of materials including organic materials[48] or liquid crystals with Δn ranging from 0.02 to 0.8.[23,49] The optic axis of the uniaxial medium is assumed to be oriented parallel to the 2D periodic plane at an angle θ with respect to Γ-K axis of the hexagonal lattice [Fig. 3(a)].

TABLE IV. $\overline{R_M}(\mathbf{k})$ for various θ and Δn in a 2D hexagonal lattice. θ_o represents an arbitrary orientation that does not coincide with any symmetrical directions of the lattice. The definition of the $\mathbf{k}$ vectors is similar to that of Table II.

		$\Delta n \neq 0$		
$\mathbf{k}$	$\Delta n=0$	$\theta=0$	$\theta=60°$	$\theta=\theta_o$
Γ	C_{6v}	C_{2v}	C_{2v}	C_2
K	C_{3v}	C_{1h}	C_{1h}	C_1
M	C_{2v}	C_2	C_{2v}	C_2
J	C_{1h}	C_1	C_{1h}	C_1
T	C_{1h}	C_{1h}	C_1	C_1
Σ	C_{1h}	C_1	C_{1h}	C_1
L	C_1	C_1	C_1	C_1

The definition of $\overline{R_M}(\mathbf{k})$ for an hexagonal lattice for $\Delta n=0$ and $\Delta n \neq 0$ is given in Table IV. In the following, we shall analyze the symmetry when the material's anisotropy is switched off ($\Delta n=0$) and switched on ($\Delta n \neq 0$).

Although we choose a materially anisotropic PC to study, the conclusion also applies for geometrically anisotropic PCs. In the geometrical anisotropic PC, the geometrical orientation of the motif is equivalent to the optic axis orientation. A specific example of the symmetry representation in a geometrically anisotropic 2D PC will be discussed in the end of Sec. IV B 1.

A. Symmetry in the absence of a spatial modulation

In the absence of a spatial modulation (or a vanishingly small refractive index modulation), the photonic band structure must reduce to a free photon dispersion with the band folding effect taken into account.[34,37,38] Assuming $\mathbf{k}=\lfloor k_x\ k_y \rfloor$ and $\mathbf{G}=\lfloor G_x\ G_y \rfloor$, Eq. (3) for H polarization in the absence of a spatial modulation and $\theta=0$ reduces to[50]

$$\frac{(k_x+G_x)^2}{n_x^2}+\frac{(k_y+G_y)^2}{n_y^2}=\left(\frac{2\pi}{a}\omega\right)^2, \tag{18}$$

where $n_x=n$ and $n_y=n+\Delta n$, with (x,y) as the periodic plane, a as the period of the PC, and ω as the normalized frequency (i.e., a divide by the free space wavelength). For E polarization, Eq. (3) reduces to $(k_x+G_x)^2+(k_y+G_y)^2=(2\pi n_z\omega/a)^2$, with $n_z=n$.[50] The terms n_x, n_y, and n_z represent the principal refractive indices of the anisotropic medium.

By using $\mathbf{G}=(2\pi n_1/a)(1,-1/\sqrt{3})+(2\pi n_2/a)(0,2/\sqrt{3})$, where (n_1,n_2) is a pair of integer that indices the reciprocal lattice point, the dispersion of a free photon with H polarization, $\omega_{free}(\mathbf{k})$ can be deduced from Eq. (18),

$$\omega_{free}(\mathbf{k})=\frac{1}{n_y}\sqrt{C_1M_{is}+C_2(r_n^2-1)M_{anis}+C_3k_xM_{k_x}+C_4k_yM_{k_y}+C_5(r_n^2-1)k_xM_{anis-k_x}+C_6}, \tag{19}$$

where $r_n=n_y/n_x$, whereas C_1, C_2, C_3, C_4, C_5, and C_6, are $\mathbf{k}$-dependent constants, and M_{is}, M_{anis}, M_{k_x}, M_{k_y}, and M_{anis-k_x} are discrete integers, which are independent of r_n and $\mathbf{k}$. For E polarization, the dispersion is also governed by an equation similar to Eq. (19), but in a simpler form with $M_{anis}=M_{anis-k_x}=0$. In order to illustrate the effect of the material's anisotropy to the dispersion of the PC, we consider only the H polarization in the rest of the paper. Nevertheless, the discussion for E polarization can be manipulated in a similar manner by setting $r_n=1$.

As degenerate states occur only at the symmetrical points of the lattice, Eq. (19) for the symmetrical points of the hexagonal lattice can be simplified as

$$\omega_{free}(\mathbf{k})=\frac{1}{n_y\sqrt{3}}\sqrt{c_1m_{is}+c_2(r_n^2-1)m_{anis}+\omega_c}, \tag{20}$$

where c_1, c_2, and ω_c are constants, whereas m_{is} and m_{anis} are discrete integers. The expressions c_1, c_2, ω_c, m_{is}, and m_{anis} at the symmetrical points of the 2D hexagonal lattice [Γ, K, K', M, and M', Fig. 3(a)] are tabulated in Table V. As we can see from Table V the distinction between K and K' as well as M and M' only occurs in their expression for m_{anis}. In the absence of the anisotropy, K and K' (M and M') are essentially equivalent points. On the other hand, it is worth mentioning that the free photon relationship of a 2D square lat-

TABLE V. Definitions of c_1, m_{is}, c_2, m_{anis}, and ω_c in Eq. (20).

$\mathbf{k}$	c_1	m_{is}	c_2	m_{anis}	ω_c
Γ	4	$n_1^2+n_2^2-n_1n_2$	3	n_1^2	0
K, K'	4	$n_1^2+n_2^2-n_1n_2+n_1$	$\frac{1}{3}$	$(3n_1+2)^2(K)$ $(3n_1+1)^2(K')$	$\frac{4}{3}$
M, M'	2	$2n_1^2+2n_2^2-2n_1n_2+2n_1-n_2$	$\frac{3}{4}$	$(2n_1+1)^2(M)$ $n_1^2(M')$	1

TABLE VI. The discrete values of m_{is} and the corresponding allowed values of m_{anis} [Eq. (20)] at Γ point. The integer in parentheses indicates n_s of the state.

Γ												
m_{is}	0 (1)	1 (6)		3 (6)		4 (6)		7 (12)			9 (6)	
$\sqrt{m_{anis}}=\lvert n_1\rvert$	0 (1)	0 (2)	1 (4)	1 (4)	2 (2)	0 (2)	2 (4)	1 (4)	2 (4)	3 (4)	0 (2)	3 (4)

tice with H polarization is also governed by an equation similar to Eq. (20) and the corresponding details are given in Appendix A.

In Eq. (20), both m_{is} and m_{anis} are discrete integers that are independent of r_n. Each state at the symmetrical points can be labeled with these integers. In the absence of an anisotropy, i.e., $\Delta n=0$ [$r_n=1$ in Eq. (20)], $\omega_{free}(\mathbf{k})$ only depends on m_{is}, and thus, the corresponding frequency levels can be labeled by using m_{is} only. As a small anisotropy is introduced (i.e., $\Delta n\neq 0$ and hence $r_n\neq 1$), each state with distinct m_{is} label will split into states with different m_{anis}. Thus, in the presence of the anisotropy, each state has to be identified by a pair of indices (m_{is},m_{anis}). The degeneracy of a state n_s with a frequency of $\omega_{free}(\mathbf{k})$ can be determined by finding the number of possible combinations of n_1 and n_2 that leads to the same (m_{is},m_{anis}). As we can see from Table V m_{anis} is a square integer. Thus, we can equivalently use $(m_{is},\sqrt{m_{anis}})$ to identify a state in the presence of the anisotropy. The possible values of m_{is} and m_{anis} and the corresponding degeneracy are listed in Tables VI–VIII for $\mathbf{k}$ vectors Γ, K, and M respectively.

For instance, at Γ point $m_{is}=n_2^2+n_1^2-n_1n_2$ (Table V), which is an integer with the first six values of 0, 1, 3, 4, 7, and 9. The degeneracy (n_s) for the first six states is 6 except for $m_{is}=0$ and $m_{is}=7$, where we have $n_s=1$ and $n_s=12$, respectively (Table VI). Other possible values of n_s at Γ must be in the multiples of 6. As a small anisotropy is introduced, each m_{is} state will split into states with different $m_{anis}=n_1^2$ (Table V). For $m_{is}=1$, the possible values of $\sqrt{m_{anis}}$ are 0 and 1 (Table VI). Hence, the corresponding state with $m_{is}=1$ $(n_s=6)$ splits into two states labeled by $m_{anis}=0$ $(n_s=2)$ and $m_{anis}=1$ $(n_s=4)$ (Table VI) as the anisotropy is introduced. If $m_{is}=7$, the degeneracy is 12 when $\Delta n=0$. When $\Delta n\neq 0$, the state $m_{is}=7$ splits into three states, each with degeneracy of 4 and $\sqrt{m_{anis}}$ of 1, 2 and 3, respectively (Table VI).

If ω is varied with respect to a parameter p such that $\omega(p)$ is a continuous function, then instead of a single state, we have a continuum of states. A band index[37] for $\omega_1(p)$ is lower than $\omega_2(p)$ provided that $\omega_1(p)<\omega_2(p)$. If $p=\Delta n$, the corresponding $\omega(p)$ given by Eq. (19) can be verified to be a continuous and a differentiable function of Δn for all real values of Δn. The $\omega(\Delta n)$ functions $(n=1.6)$ with the corresponding $(m_{is},\sqrt{m_{anis}})$ labels are plotted at Γ point and K point in Figs. 5(a) and 5(b), respectively. As we can see from the figure, in the absence of the anisotropy, a lower band essentially has a lower value of m_{is}. However, when an anisotropy is introduced, such a correspondence is generally invalid. For instance, in Fig. 5(a) when Δn is between −0.4 and 0, the states (4, 2) have larger frequency than (3, 1). When $\Delta n=0.4$, the two states have a common frequency and when $\Delta n<-0.4$, the frequency of (3, 1) leads that of (4, 2). The exact value of r_n^2 (or Δn), where any two states with $(m_{is},\sqrt{m_{anis}})$ label $(a_{is},\sqrt{a_{anis}})$ and $(b_{is},\sqrt{b_{anis}})$ will meet at a common frequency can be obtained from Eq. (20),

$$r_n^2=1-\frac{c_1(a_{is}-b_{is})}{c_2(a_{anis}-b_{anis})}. \tag{21}$$

It is clear from Eq. (21) that states with the same m_{is} will not cross unless $r_n=1$ and crossing between states with the same m_{anis} is not allowed.

The eigenmode symmetry of each degenerate state $(m_{is},\sqrt{m_{anis}})$ is described by a reducible representation, and the characters of such representations (i.e., trace of representation matrix[43,44]) are independent of r_n. The dimension of the representation in each state is given by n_s of the state and the corresponding characters of the representation can be found by using the procedure outlined in Refs. 34 and 37. By using the standard group theory reduction procedure,[43,44] the representation can be written as a direct sum of IR of $\bar{R}_M(\mathbf{k})$ [see Table IV for definitions of $\bar{R}_M(\mathbf{k})$]. The result of such an analysis is presented in Table IX by noting that symbols A_1, A_2, B_1, B_2, A, and B refer to different 1D IRs in Muliken's notation, whereas E_1 and E_2 refer to different 2D IRs in Muliken's notation. More detailed information on these symbols can be found in Ref. 33, 43, and 44.

B. Symmetry in the presence of spatial modulation

As the spatial modulation is switched on, the degenerate states in Tables VI–IX split into states, which can be further labeled by an IR of $\bar{R}_M(\mathbf{k})$. If the modulation is increased such that the symmetry of $\bar{R}_M(\mathbf{k})$ in the absence of the spatial modulation is retained, then the corresponding state will split according to the IRs of $\bar{R}_M(\mathbf{k})$ in the absence of spatial

TABLE VII. The discrete values of m_{is} and the corresponding allowed values of m_{anis} [Eq. (20)] at K point. The integer in parentheses denotes n_s of the state.

K												
m_{is}	0 (3)		1 (3)		2 (6)			4 (6)			5 (3)	
$\sqrt{m_{anis}}=\lvert 3n_1+2\rvert$	1 (2)	2 (1)	2 (2)	4 (1)	1 (2)	4 (2)	5 (2)	2 (2)	5 (2)	7 (2)	4 (2)	8 (1)

TABLE VIII. The discrete values of m_{is} and the corresponding allowed values of m_{anis} [Eq. (20)] at M point. The integer in parentheses denotes n_s of the state.

	M									
m_{is}	0 (2)	1 (2)	3 (4)		4 (2)	6 (4)		9 (4)		
$\sqrt{m_{anis}}=\lvert 2n_1+1\rvert$	1 (2)	1 (2)	1 (2)	3 (2)	3 (2)	1 (2)	3 (2)	3 (2)	5 (2)	

modulation. If the increase in the modulation reduces the number of symmetry elements in $R_M(\mathbf{k})$ [i.e., $R_M(\mathbf{k})$ in the presence of modulation is a subgroup of the one in the absence of spatial modulation), then the corresponding IR have to be subduced[43,44] from the IRs of $R_M(\mathbf{k})$ in the absence of the spatial modulation.

In the presence of the spatial modulation, the solutions to Eq. (3) can be obtained by means of a plane wave expansion,[37,45,51,52] in which the eigenfunction is expanded into a set of basis functions, i.e., plane waves. Eigenvalues with a particular IR can be obtained by only selecting the basis functions of this IR.[38,43,44,52] If the dispersion relation, $\omega(p)$ is a continuous and differentiable function of p, and the group $R_M(\mathbf{k})$ does not change as p changes, then a small change in p only causes a small change in the value of ω and has no effect on the symmetry of the eigenmode. Thus, the eigenmodes of the $\omega(p)$ function with the same $R_M(\mathbf{k})$ will have the same IR.

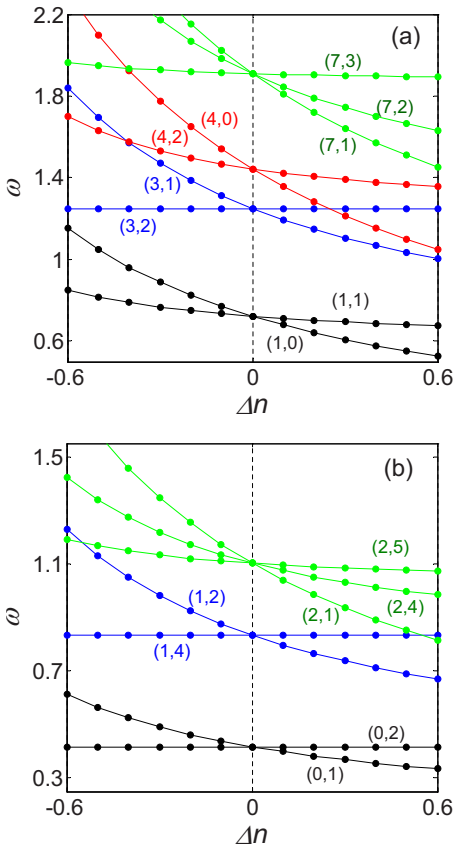

FIG. 5. (Color online) Splitting of degenerate states in the absence of a spatial modulation (H polarization). ω versus Δn relationship at (a) Γ point and (b) K point. The states are labeled by a pair of indices $(m_{is}, \sqrt{m_{anis}})$. Each different color represents a different m_{is}.

1. Symmetry as a function of spatial modulation

The plot of $\omega(r_c)$ at Γ point, with $n=1.6$, $\Delta n=0.6$, and $\theta=0$, is given in Fig. 6. The figure shows the splitting of degenerate states $(m_{is}=1, \sqrt{m_{anis}}=0)$ and $(m_{is}=1, \sqrt{m_{anis}}=1)$ as a function of r_c. The first degenerate state $(m_{is}=1, \sqrt{m_{anis}}=0)$ in Fig. 6 has a representation $A_1 \oplus B_2$ (Table IX). The symbol $\oplus$ indicates that the representation is reducible and composes two 1D IRs, A_1 and B_2. As the spatial modulation is switched on, the state splits into two states, which form two continuous and differentiable $\omega(r_c)$ functions as r_c is varied. The symmetry of the eigenmodes at any r_c for the same function is the same, and hence, these two functions can be written as $\omega_{A_1}(r_c)$ and $\omega_{B_2}(r_c)$ with the symmetry of the eigenmodes at any r_c is given by the IRs, A_1 and B_2, respectively.

The definition of a band[37] that indices a lower frequency with a lower index and an higher frequency with an higher index causes a little confusion. That is, when $\omega_{A_1}(r_c)$ and $\omega_{B_2}(r_c)$ cross, the two bands interchange the symmetry. For instance, in Fig. 6, these two functions cross at $r_c=0.18$ and the respective symmetry at the left and right of the intersection point for band 1 is B_2 and A_1, respectively. This can be further verified by examining the symmetries of the numerically computed eigenmodes in Figs. 7(a) and 7(b) for $r_c=0.1$ and $r_c=0.25$, respectively. The intersection point at $r_c=0.18$ has an accidental[40,46] twofold degeneracy with a 2D

TABLE IX. Representations of degenerate states of a 2D hexagonal lattice in the absence of spatial modulation.

k	m_{is}	Representation	$\sqrt{m_{anis}}$	Representation
Γ	0	A_1	0	A_1
	1	$A_1+B_2+E_1+E_2$	0	A_1+B_2
			1	$A_1+A_2+B_1+B_2$
	3	$A_1+B_1+E_1+E_2$	1	$A_1+A_2+B_1+B_2$
			2	A_1+B_1
K	0	A_1+E	1	$A+B$
			2	A
	1	A_1+E	2	$A+B$
			4	A
	2	A_1+A_2+2E	1	$A+B$
			4	$A+B$
			5	$A+B$
M	0	A_1+B_1	1	$A+B$
	1	A_1+B_2	1	$A+B$
	3	$A_1+A_2+B_1+B_2$	1	$A+B$
			3	$A+B$

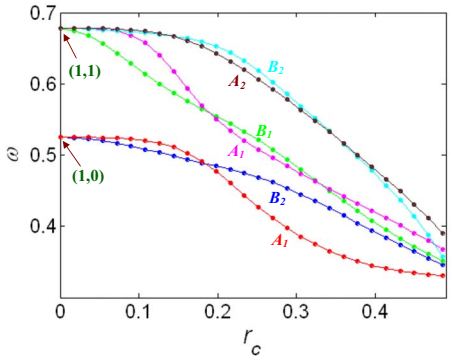

FIG. 6. (Color online) Splitting of states at Γ point as a function of r_c in a PC made of an isotropic circular cylinders with refractive index of 3.5 in an uniaxial matrix medium (H polarization, $\Delta n=0.6$, $n=1.6$, and $\theta=0$).

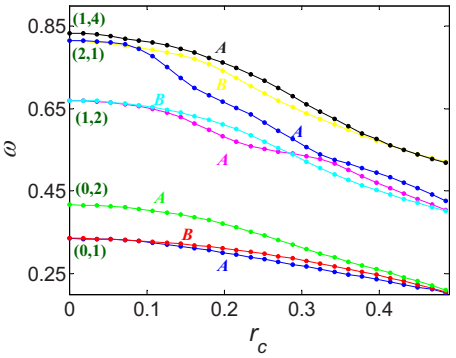

FIG. 8. (Color online) Splitting of states at K point as a function of r_c in a PC made of isotropic circular cylinders with refractive index of 3.5 in an uniaxial matrix medium (H polarization, $\Delta n=0.6$, $n=1.6$, and $\theta=0$).

reducible representation, $A_1 \oplus B_2$. The same analysis can be done for the second degenerate state when $r_c=0$, $(m_{is}=1, \sqrt{m_{anis}}=1)$. The representation of this state can be obtained from Table IX to be $A_1 \oplus A_2 \oplus B_1 \oplus B_2$, which contains four 1D IRs. Hence, there are four $\omega(r_c)$ functions with four different IRs originating from the second degenerate state $(m_{is}=1, \sqrt{m_{anis}}=1)$. The $\omega(r_c)$ plot with the symmetry assignments at K point is given in Fig. 8 for the same configuration of PC as in Fig. 6. The representation of the degenerate states $(r_c=0)$ can be obtained from Table IX, noting the state $(m_{is}=1, \sqrt{m_{anis}}=4)$ has a larger frequency than the state $(m_{is}=2, \sqrt{m_{anis}}=1)$ when $\Delta n=0.6$ [Fig. 5(b)].

In Fig. 6, all eigenmodes have only 1D IRs as $\overline{R_M}(\Gamma)=C_{2v}$ for $\Delta n \neq 0$ and $\theta=0$ (Table X). If $\overline{R_M}(\Gamma)$ is a higher order group with 2D IRs (see Table IV, for list of IRs of various R_M groups), then we will have the twofold degeneracy originating from the 2D IR retained. For example, when $\Delta n=0$, $\overline{R_M}(\Gamma)=C_{6v}$ (Table IV), the state with $m_{is}=1$ $(r_c=0)$ has a representation $A_1 \oplus B_2 \oplus E_1 \oplus E_2$ with a sixfold degeneracy (Table IX) and there are four $\omega(r_c)$ functions originating from this state, as shown in Fig. 9. The representation at $r_c=0$ contains two 1D IRs (A_1 and B_2) and two 2D IRs (E_1 and E_2), and as the increase in r_c does not disturb $\overline{R_M}(\Gamma)$, the twofold degeneracy in the $\omega_{E_1}(r_c)$ and $\omega_{E_2}(r_c)$ is retained when r_c is varied. The twofold degeneracy can be lifted up if there is a change in the $\overline{R_M}(\Gamma)$, which will be shown in Sec. IV B 2. Figure 9 also shows that as r_c increases, the symmetry at a particular band changes, and more specifically, the occurrence of degenerate band could shift. Such a shift is easily predicted using plots like Fig. 9. For instance, in Fig. 9, until $r_c=0.13$, the degenerate bands (at Γ point) are bands 1 and 3 (recall that the band index is such that a lower frequency will have a lower index and a higher frequency will have an higher index); however, for r_c values thereafter until $r_c=0.46$, the degenerate bands shift to be bands 2 and 3.

The ω versus r_c relationship for an inverse structure, in which the matrix medium is isotropic and the cylinders are uniaxially anisotropic, is different with the direct structure, in which the matrix is anisotropic and the cylinders are isotropic. The $\omega(r_c)$ plot at Γ point is shown in Fig. 10 for the inverse structure with $\Delta n=0.6$ and $\theta=0$, which can be compared with Fig. 6 (direct structure). Unlike the direct structure where we do not have any sixfold degenerate points for $r_c=0$, the inverse structure has a sixfold degenerate point when $r_c=0$. This is because the inverse structure has $\overline{R_M}(\Gamma)=C_{6v}$ in the limit of zero modulation. Thus, its dispersion in the absence of a spatial modulation is similar to that of an isotropic medium, and hence, the corresponding degenerate states for $r_c=0$ can be labeled by using m_{is} only. A small increase in r_c lowers the symmetry of $\overline{R_M}(\Gamma)$ from C_{6v} to its subgroup C_{2v}. From Table IX, when $m_{is}=1$ $(r_c=0)$, we have a representation $A_1 \oplus B_2 \oplus E_1 \oplus E_2$ (a sum of IRs of

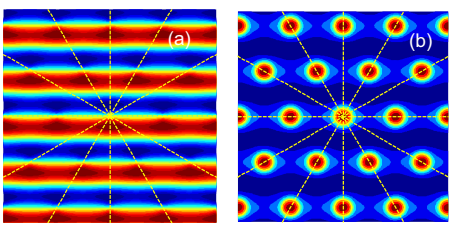

FIG. 7. (Color online) Magnetic field pattern associated with eigenmodes of the first band (with nonzero frequency) at Γ point of a PC made of isotropic circular cylinders with refractive index of 3.5 in an uniaxial matrix medium (H polarization, $\Delta n=0.6$, $n=1.6$, and $\theta=0$) when r_c equals (a) 0.1 and (b) 0.25.

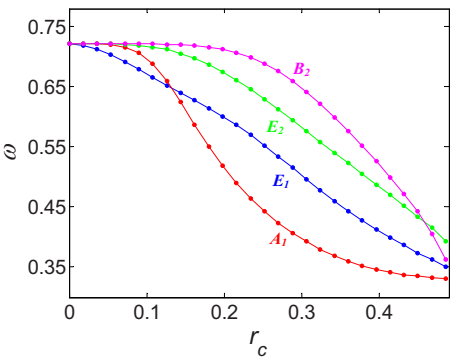

FIG. 9. (Color online) Splitting of states at Γ point as a function of r_c in a PC made of isotropic circular cylinders with refractive index of 3.5 in an isotropic matrix medium of refractive 1.6 (H polarization). The degenerate state at $r_c=0$ has $m_{is}=1$.

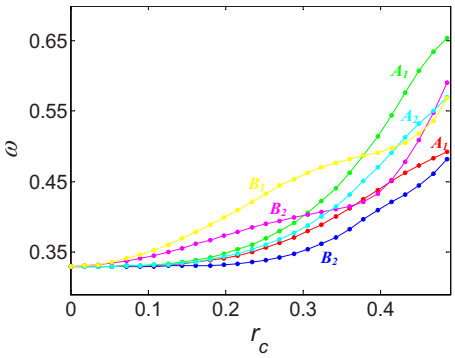

FIG. 10. (Color online) Splitting of states at Γ point as a function of r_c in a PC made of uniaxial circular cylinders (H polarization, $\Delta n=0.6$, $n=1.6$, and $\theta=0$) in an isotropic matrix medium with refractive index of 3.5. The degenerate state at $r_c=0$ has $m_{is}=1$.

C_{6v}). However, for a very small nonzero r_c, this representation becomes a subduced representation[54] and using the reduction procedure,[43,44] the representation can be written as a sum of IRs of C_{2v}, $2A_1 \oplus 2B_2 \oplus A_2 \oplus B_1$. Thus, there are six $\omega(r_c)$ functions [$2\omega_{A_1}(r_c)$, $2\omega_{B_2}(r_c)$, $\omega_{A_2}(r_c)$, and $\omega_{B_1}(r_c)$] in Fig. 10.

It is worth mentioning that for a geometrically anisotropic 2D PC (i.e., no material's anisotropy), the splitting of the states will be similar to the one in Fig. 10 as long as their $\overline{R_M}(\Gamma)$ in the presence and the absence of a spatial modulation is C_{6v} and C_{2v}, respectively. For example, considering a square motif with an area A_c in an hexagonal lattice PC with the orientation of the motif matching the symmetrical axes of the lattice (Table I), if we assume the background to be an isotropic material, then in the limit of $A_c \to 0$, $\overline{R_M}(\Gamma)=C_{6v}$. For a very small but a nonzero A_c, we have $\overline{R_M}(\Gamma)=C_{2v}$.

2. Symmetry as a function of the anisotropy

It can be easily verified that the compatibility of the symmetry between Fig. 6 [$\Delta n \neq 0$, $\overline{R_M}(\Gamma)=C_{2v}$] and Fig. 9 [$\Delta n=0$, $\overline{R_M}(\Gamma)=C_{6v}$] is somehow missing. For instance, in Fig. 9, when $r_c=0.25$, bands 1, 2, 3 and 4 has an IR of A_1, E_1, E_2, and B_2, respectively. When the anisotropy is switched on, $\overline{R_M}(\Gamma)=C_{2v}$, having only 1D IRs (Table X), and therefore, the degenerate functions in Fig. 9 [i.e., $\omega_{E_1}(r_c)$ and $\omega_{E_2}(r_c)$] split, and in total, there are six ω functions in Fig. 6. When $r_c=0.25$, band 1, 2, 3, 4, 5 and 6 has an IR A_1, B_2, A_1, B_1, A_2 and B_2, respectively (Fig. 6). From the compatibility relation between groups C_{6v} and C_{2v} (Table XI), the IR A_1 of C_{6v} is compatible with that of A_1 of C_{2v}. This compatibility matches with symmetry representations at band 1 ($r_c=0.25$) of Figs. 6 and 9, as both have symmetry labeled by A_1. However, the compatibility between these figures is missing for bands 2 and 3. From the compatibility relation between groups C_{6v} and C_{2v} (Table XI), E_1 (IR of C_{6v}) is only compatible with B_1 and B_2 (IRs of C_{2v}). This means that the degenerate band, E_1 for $\overline{R_M}(\Gamma)=C_{6v}$ will split into bands with IRs B_1 and B_2 for $\overline{R_M}(\Gamma)=C_{2v}$. However, band 2 ($r_c=0.25$), with IR, E_1 in Fig. 9, seems to be splitted into bands with IR, B_2 (band 2, $r_c=0.25$) and A_1 (band 3, $r_c=0.25$) in Fig. 6. Such a noncompatibility is a consequence of a drastic change in the anisotropy [i.e., $\Delta n=0$ in Fig. 9 and $\Delta n=0.6$ in Fig. 6]. In order to monitor the symmetry evolution, a plot of $\omega(\Delta n)$ with a continuous variation of Δn such as the one in Fig. 11 is required. From Fig. 11, we can see that the function $\omega_{E_1}(r_c)$ splits into $\omega_{B_1}(r_c)$ and $\omega_{B_2}(r_c)$ functions. However, the crossing at $\Delta n=0.45$ causes the change of the symmetry of the third band from B_1 to A_1.

TABLE X. The order, symmetry elements, and IRs of the symmetry groups compatible with the 2D hexagonal lattice. Notation of symmetry elements and IRs follows Schonflies's and Mulliken's, respectively (Refs. 37, 43, and 44). The symmetry element σ_ϕ refers to a mirror operation along an axis $y=x\tan(\phi)$ [where ϕ is defined along the anticlockwise direction from the $+x$ axis] and C_n in the symmetry element refers to n-fold rotation (anticlockwise rotation around the axis perpendicular to the 2D periodic plane). The IRs with symbols A_1, A_2, B_1, B_2, A, and B are 1D IRs, whereas E_1, E_2, E, E', and E'' are 2D IRs. For more detailed explanations on the IR symbols, please refer to Ref. 43 and 44 or any other crystallographic group theory text.

Group	Order	Symmetry elements	IRs
C_{6v}	12	E, C_2, C_3, C_3^{-1}, C60$_6$, C_6^{-1}, σ_{-60°, σ_{-30°, σ_{0°, σ_{30°, σ_{60°, σ_{90°	A_1, A_2, B_1, B_2, E_1, E_2
C_{3v}	6	E, C_3, C_3^{-1}, σ_{-60°, σ_{0°, σ_{60°	A_1, A_2, E
C_{2v}	4	E, C_2, σ_{0°, σ_{90°	A_1, A_2, B_1, B_2
C_6	6	E, C_2, C_3, C_3^{-1}, C_6, C_6^{-1}	A, B, E', E''
C_3	3	E, C_3, C_3^{-1}	A, E
C_{1h}	2	E, σ_{0°	A, B
C_2	2	E, C_2	A, B
C_1	1	E	A

3. Symmetry as a function of the orientation of the motif

The symmetry of the eigenmodes and the eigenvalues vary with the orientations of the motif. As an example, the relationship between ω and θ, $\omega(\theta)$, for $\Delta n=0.6$ and $r_c=0.25$ is shown in Figs. 12(a)–12(d), respectively, for Γ, T, Σ, and L points. (The definitions of these **k** vectors can be found in Table II.)

TABLE XI. Compatibility relation between groups C_{6v}, C_{2v}, and C_2. Each column contains IRs of C_{6v} (A_1, A_2, B_1, B_2 E_1, and E_2), C_{2v} (A_1, A_2, B_1, and B_2), and C_2 (A and B). The compatibility between IRs of different groups can be obtained by examining the rows. Examples: A_1 of C_{6v} is compatible with A_1 of C_{2v} and A of C_2 (row 1), A of C_2 is compatible with A_1, A_2, or E_2 of C_{6v} (rows 1, 2, and 6), and A_1 or A_2 of C_{2v} (rows 1 and 2 or row 6).

C_{6v}	C_{2v}	C_2
A_1	A_1	A
A_2	A_2	A
B_1	B_1	B
B_2	B_2	B
E_1	B_1, B_2	B
E_2	A_1, A_2	A

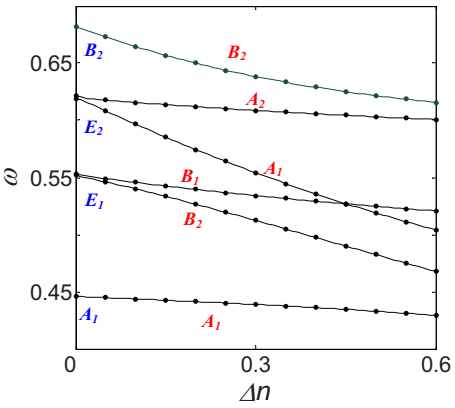

FIG. 11. (Color online) Splitting of states at Γ point as a function of Δn in a PC made of isotropic circular cylinders (r_c=0.25 and refractive index=3.5) in a uniaxial matrix medium of birefringence Δn (H polarization, n=1.6, and θ=0).

The symmetries of the eigenvalues in Fig. 12(a)–12(d) are governed by Eq. (15) and the corresponding symmetries are given by the group R_θ. The group of R_M for a general orientation is given by the group C_2 (Table I), and hence, the corresponding definition of R_θ can be found from Table II to be C_{6v}, C_{2v}, C_{2v}, and C_2, respectively, for Γ, T, Σ, and L points (the elements of these groups can be found in Tables X–XII, except for Σ point, the group C_{2v} has mirror elements $\sigma_{-30°}$ and $\sigma_{60°}$, i.e., $C_{2v'}$). The FZO of these R_θ groups can be identified from Fig. 4 and Table III. As we mentioned in Sec. III B, only eigenvalues within a FZO are unique and this can be readily verified from $\omega(\theta)$ plots in Figs. 12(a)–12(d). Similarly, the eigenfunctions remain distinct only for the orientations within a FZO. The corresponding assignment of IRs to the eigenmodes within a FZO is shown in Figs. 12(a)–12(d).

As θ variation is continuous, the assignment of IR of $R_M(\mathbf{k})$ to the eigenmodes of $\omega(\theta)$ can be done by using compatibility relations. Compatibility relations between groups C_{6v}, C_{2v}, and C_2 are given in Table XI and the complete tables of compatibility relationships between crystallographic point groups can be obtained from Refs. 43 and 44.

In Fig. 12(a) (Γ point) when θ=0, $R_M(\Gamma)=C_{2v}$, the corresponding symmetry assignments at each band can be obtained from Fig. 6 at r_c=0.25. For a small change in θ, $R_M(\Gamma)=C_2$, the corresponding symmetry assignment can be done with the aid of compatibility relation between C_{2v} and C_2 (Table XI). For example, when θ=0 $[R_M(\Gamma)=C_{2v}]$, the symmetry representation of the first band is labeled with IR of C_{2v} A_1 (obtained from Fig. 6 at r_c=0.25). For a small change in θ $[R_M(\Gamma)=C_2]$, the symmetry representation must be compatible with the IR of C_{2v}, A_1. From Table XI, we know A_1 (IR of C_{2v}) is compatible with the IR A of C_2.

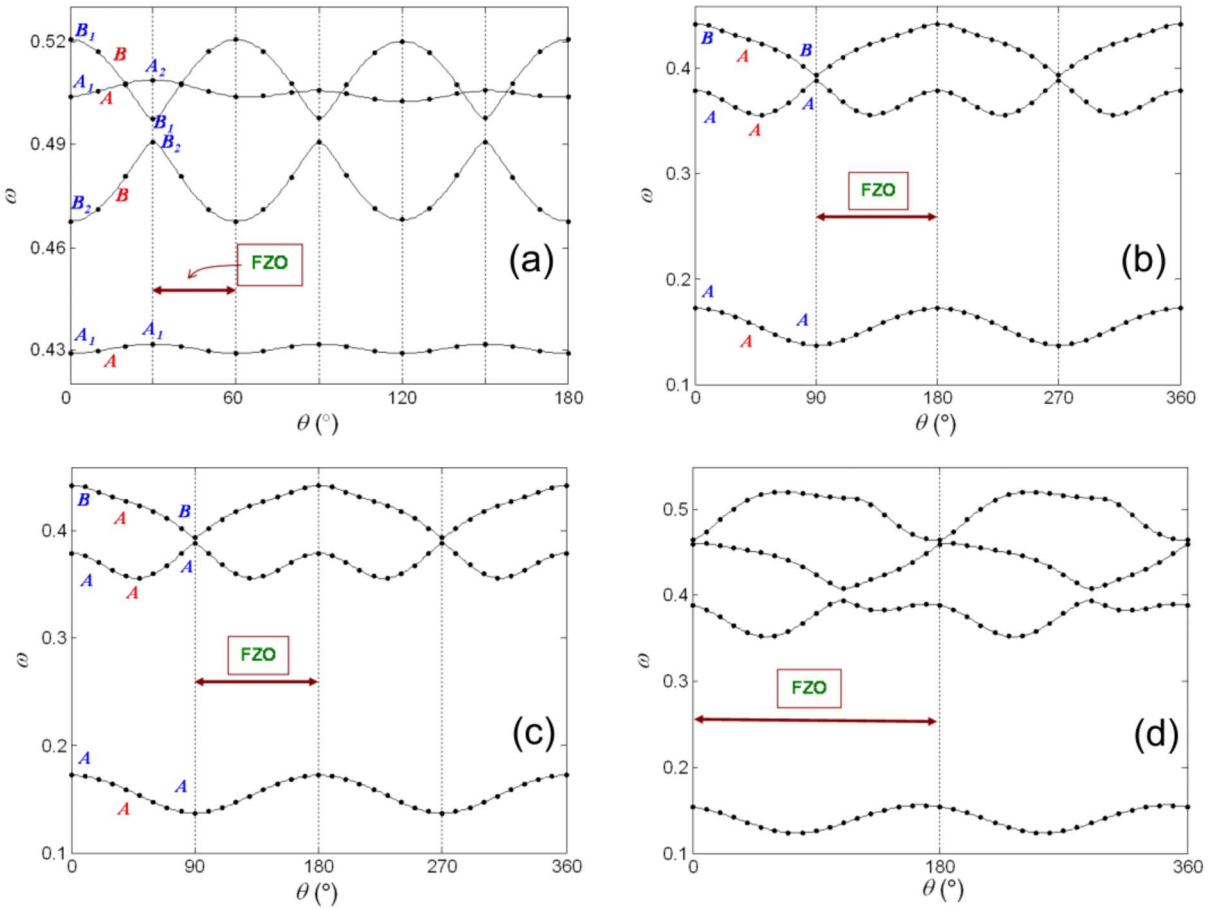

FIG. 12. (Color online) ω as a function of θ, in a PC made of isotropic circular cylinders (r_c=0.25 and refractive index=3.5) in a uniaxial matrix medium (H polarization, Δn=0.6, and θ=0) at $\mathbf{k}$ vectors (a) Γ, (b) T (mid of ΓK), (c) Σ (mid of ΓM), and (d) L (mid of ΓJ).

Therefore, for a small change in θ, the symmetry representation of the band 1 is labeled with the IR, A of C_2. Thereafter, a continuous variation of θ in $0<\theta<30°$ causes the whole continuous function of $\omega(\theta)$ $(0<\theta<30°)$ to possess the same IR, as such, a variation of θ does not alter the group, $\overline{R_M}(\Gamma)$. As observed in Fig. 6 for $\omega(r_c)$ functions, if two $\omega(\theta)$ functions of different IRs cross, the bands exchange the symmetry at the intersection point. When $\theta=30°$, $\overline{R_M}(\Gamma)=C_{2v}$, the compatibility relations (Table XI) show that a single IR of a group C_2 is compatible with more than one IR of C_{2v}. Thus, a numerical examination of the eigenfunction is also necessary in this case. The IR assignment of other **k** vectors follow a similar approach and is presented within the FZO in Figs. 12(b)–12(d). In Fig. 12(d), as $\overline{R_M}(\mathrm{L})=C_1$, all eigenmodes have an IR A (Table XI).

As we have mentioned in Sec. III B, the equivalent orientations have rotated versions of the eigenfunctions, although the symmetry representation of eigenmodes at equivalent orientations necessarily has the same set of characters, which refers to the trace of the representation matrix and does not altered by orthogonal transformations (i.e., rotations).[43,44] The eigenmodes of band 3 at the equivalent orientations, $\theta=0°$, 60°, and 120° are shown in Figs. 13(a)–13(c), respectively. As we can see from these figures, all equivalent orientations have A_1 symmetry, but the eigenfunctions are rotated. When $\theta=180°$, $R_\theta=C_2\in\overline{R_M}(\mathbf{k})$, $R_\theta\mathbf{H_k}(\mathbf{r})=\mathbf{H_k}(\mathbf{r})$, and hence, we have the same eigenfunction as when $\theta=0$.

V. DISCUSSIONS AND IMPLICATIONS

This section summarizes the important results of the paper and discusses how these results can be applied in the design of anisotropic PCs. In Sec. II, important symmetry groups that is relevant to anisotropic PCs were defined. The collection of all symmetry elements of the operator M in an anisotropic PC with symmorphic space group $\overline{G_M}$ can be expressed as $\overline{G_M}=\bar{T}\otimes\overline{R_M}$, where $\overline{R_M}$ is a subgroup of $\bar{R}$ $(\overline{R_M}=\bar{R}\cap\overline{R_B})$.

Section III discusses the symmetries in the wave equation and contains subsections devoted to theoretical formulations of IBZ and FZO of anisotropic PCs. Section III A describes the IBZ of an anisotropic PC. The symmetry elements of group $\bar{R}$ reduces the BZ to an IBZ. This IBZ is defined as the IBZ of the lattice. On the other hand, the symmetry elements of group $\overline{R_M}$ reduces BZ to the IBZ of the anisotropic PC. The relationship between IBZ of the lattice and IBZ of the anisotropic PC is defined through the coset expansion of $\bar{R}$ with respect to $\overline{R_M}$ and it is shown that the ratio of the size of the IBZ of the lattice to the size of the IBZ of the anisotropic PC must be an integer and equals to r/r_m. The IBZ of the lattice is fixed for a given lattice and can be found in the standard literatures and textbooks.[43,53] Once the IBZ of a lattice is known, we can obtain the IBZ of the anisotropic PC by transforming the wave vectors in the IBZ of the lattice by using the r/r_m number of symmetry operations R, where R is chosen from each coset of $\bar{R}$ expanded with respect to $\overline{R_M}$. The usefulness of an IBZ is well known as it defines the smallest zone of **k** vectors in the reciprocal space for which the eigenvalues are unique. The complete information regarding photonic band gaps and equal frequency surfaces[4] can be obtained by only manipulating the **k** vectors within the IBZ. Therefore, the presented method to identify the IBZ of an anisotropic PC will be useful in the calculation of the photonic band gaps[8–24,26,28,30,31] and equal frequency surfaces[25,27,55,56] of the anisotropic PC.

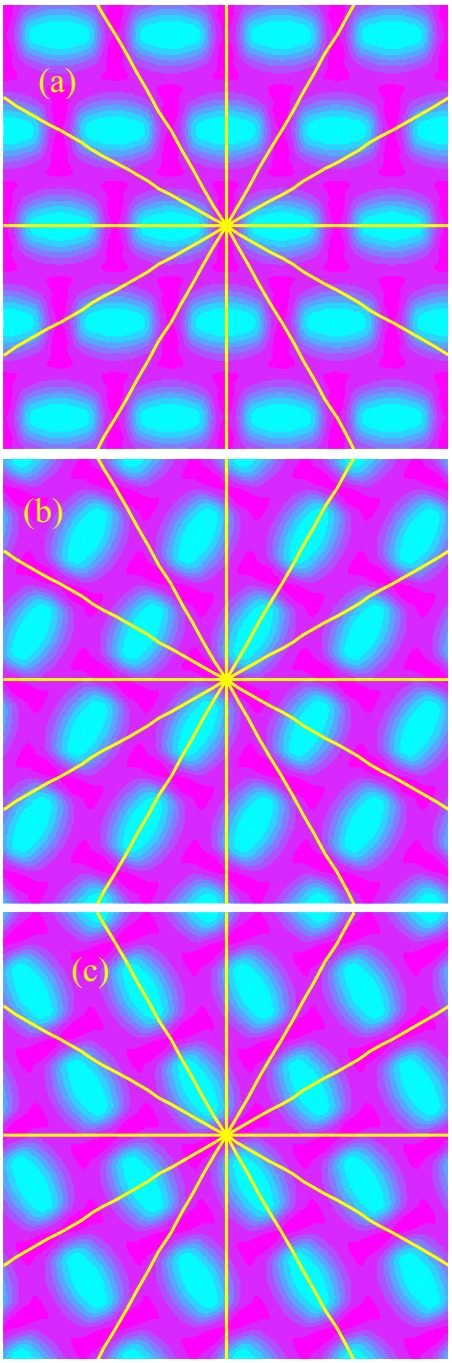

FIG. 13. (Color online) Magnetic field pattern associated with eigenmodes of equivalent orientations at the third band in a PC made of isotropic circular cylinders ($r_c=0.25$ and refractive index $=3.5$) in a uniaxial matrix medium (H polarization, $\Delta n=0.6$, and $\theta=0$) at Γ point. (a) $\theta=0$ and 180°, (b) $\theta=60°$, and (c) $\theta=120°$.

Section III B introduced the concepts of orientational group and FZO. Orientational group $\overline{R_\theta}$ consists of orienta-

tional symmetry operations, $R_\theta = R_M R$, with $R_M \in \overline{R_M}$ of general orientation and $R \in \bar{R}(\mathbf{k})$. If all possible orientations of motif are represented as a zone (an unit circle for a 2D PC and an unit sphere for a 3D PC), the existence of orientational symmetry reduces the zone to a FZO, where only the orientations within the FZO have unique eigenvalues [Eq. (3)]. The difference (and similarity) between IBZ and FZO of an anisotropic PC is that the IBZ of an anisotropic PC is a reduced zone of **k** vectors (because of the symmetries in the $\overline{R_M}$), for which the eigenvalue of Eq. (3) remain unique at a particular orientation of the motif, whereas FZO is a reduced zone of orientations (because of the symmetries in the $\overline{R_\theta}$), for which the eigenvalue of Eq. (3) remain unique at a particular **k** vector.

In the design of anisotropic PCs, FZO plays an important role. For example, optical properties such as curvatures of equal frequency surface near a particular **k** vector (important for dispersive effect such as superprism[25]) and direction dependent band gaps (i.e., **k** dependant) varies with the motif orientations, and therefore, the range of orientations for which the optical properties remain unique is essentially governed by FZO. Hence, in applications such as optimizing the band gap with respect to orientations of the anisotropic motif,[11,13,18] FZO limits the unique orientations that could be explored for optimization. In some materially anisotropic PCs such as LC infiltrated PCs, the tunability of band gaps[21–24,28,30] or any other dispersive effects[25,27] are obtained by means of reorientating optic axis under an external electric field. In these applications, the tuning range (the range of orientations of optic axis for which the tunability is unique) of direction dependent band gaps varies with different directions of the lattice. Such a tuning range can be easily manipulated by finding the FZO at the particular **k** vector. Instead of band gap at a single **k** vector, if the overall band gap corresponding to a range of **k** vectors (with different **k** vectors have different FZO) is to be monitored as a function of motif orientation, the corresponding symmetry in the motif orientation for the overall bandgap will be governed by the smallest FZO.

Section IV discusses the symmetry of the eigenmodes in a 2D anisotropic PC with hexagonal lattice. In particular, we choose a structure with the matrix medium being uniaxially anisotropic with $\theta=0$. We started with the discussion of labeling the system and symmetry representation in the absence of spatial modulation. By using Eq. (20), the degenerate states at symmetrical **k** can be labeled by using an integer m_{is} in the absence of spatial modulation and material's anisotropy. If material's anisotropy is present, the state with the label m_{is} will split into states that can be further identified with a label of $\sqrt{m_{anis}}$. Symmetry representation of each state labeled by a pair of integers $(m_{is}, \sqrt{m_{anis}})$ is described by a reducible representation, which is independent of the strength of material's anisotropy (i.e., independent of r_n). The definition of m_{is} and m_{anis} and the possible values are described in Tables V–VIII, respectively.

The labeling system provides an analytical guideline in determining the degeneracy, explicit frequency levels, crossings between states, effect of material anisotropy to the splitting of degenerate states, and the representation of a degenerate state in the absence of spatial modulation. Apart from this, the labeling system and the integers (m_{is} and m_{anis}) help in getting analytical description for the evolution of the states in the presence of spatial modulation.[57] Furthermore, these integers derived from the free photon relationship of a PC and the corresponding degeneracies allow us to predict diffraction conditions and the number of diffracted spots (equals to degeneracy of the state) of a very weakly modulated anisotropic PC (i.e., diffraction grating) as the dispersion in such a structure is essentially free photon dispersion with the band folding effect taken into account. In weakly modulated isotropic PCs, every m_{is} corresponds to a diffraction order. Following Eq. (20), we can show that for isotropic PC ($r_n=1$), the condition for the first order diffraction ($m_{is}=1$) at the symmetrical **k** point of hexagonal lattice is $3n^2\omega^2 > 2/3$, and there will be six diffracted spots (since the degeneracy of the state $m_{is}=1$ is 6). The details of diffraction and the experiment for weakly modulated isotropic PCs has been presented by us based on Γ point.[58] In a weakly anisotropic PC [with uniaxial anisotropic matrix ($\theta=0$)], the diffraction order must be identified with $(m_{is}, \sqrt{m_{anis}})$, and the corresponding diffraction condition will be $3n_y^2\omega^2 > c_1 m_{is} + c_2(r_n^2-1)m_{anis} + \omega_c$ [Eq. (20)], and the degeneracy of the state $(m_{is}, \sqrt{m_{anis}})$ (Tables VI–VIII) will equal the number of diffracted spots.

As the spatial modulation is switched on, the degenerate states in the absence of spatial modulation split into states which can be further labeled by the IRs of $\overline{R_M}(\mathbf{k})$. The degeneracy in the presence of spatial modulation is determined by the dimension of the IR that labels the eigenvalue. Understanding of symmetry representations of the eigenmodes of a PC has great importance as the coupling efficiency of light from an external source to the PC essentially depends on the eigenmode symmetry of PC.[34–36] The degeneracy in the presence of spatial modulation is very useful in engineering the band gap of an anisotropic PC.[18–20] In this paper, we have presented the details of symmetry representation for a 2D PC with circular air holes in the uniaxial matrix medium for a continuous variation of spatial modulation (i.e., r_c), material's anisotropy (i.e., Δn), and the orientation of the motif (i.e., θ).

In the 2D PC with a uniaxial anisotropic matrix ($\theta=0$) and circular isotropic holes (i.e., air), the symmetry representation in the absence of spatial modulation at each degenerate state labeled with $(m_{is}, \sqrt{m_{anis}})$ is expressed by a reducible presentation [i.e., a sum of IRs of $\overline{R_M}(\mathbf{k})$, see Table IX]. The introduction of spatial modulation (i.e., circular air holes) does not alter the group $\overline{R_M}(\mathbf{k})$, and the state $(m_{is}, \sqrt{m_{anis}})$ splits into states, which can be further labeled by IRs of $\overline{R_M}(\mathbf{k})$.

On the other hand, in the 2D PC with isotropic matrix and circular holes of uniaxial media ($\theta=0$), the symmetry representation in the absence of spatial modulation at each degenerate state is labeled by m_{is} alone, which is again expressed by a reducible presentation. However, in this case, the introduction of spatial modulation will change the group $\overline{R_M}(\mathbf{k})$ [i.e., $\overline{R_M}(\mathbf{k})$ in the presence of modulation is a subgroup of the one in the absence of modulation] and the symmetry representation for a nonzero r_c therefore has to be subduced from the IRs of $\overline{R_M}(\mathbf{k})$ in the absence of modulation. The

TABLE XII. Definitions of c_1, m_{is}, c_2, m_{anis}, and ω_c in Eq. (A1).

k	c_1	m_{is}	c_2	m_{anis}	ω_c
Γ (0,0)	1	$n_1^2+n_2^2$	1	n_1^2	0
M $(\pi/a,\pi/a)$	1	$n_1^2+n_2^2+n_1+n_2$	$\frac{1}{4}$	$(2n_1+1)^2$	$\frac{1}{2}$
X $(\pi/a,0)$	1	$n_1^2+n_2^2+n_1$	$\frac{1}{4}$	$(2n_1+1)^2$	$\frac{1}{4}$

same situation applies for any geometrically anisotropic PC with all isotropic materials. The introduction of geometrically anisotropic motif will lower the symmetry, and consequently, $R_M(\mathbf{k})$ in the absence of spatial modulation changes to its subgroup when the spatial modulation is switched on.

Apart from the symmetry representations of the eigenmodes, the paper also discusses the degeneracy in the presence of spatial modulation. In the presence of spatial modulation, when the material anisotropy is varied (i.e., Δn), from zero to a nonzero value, the $R_M(\mathbf{k})$ group is altered. We have given the details of symmetry representation at Γ point of the hexagonal lattice. The group $R_M(\Gamma)$ with $\theta=0$ is C_{6v} and C_{2v}, respectively, for $\Delta n=0$ and $\Delta n\neq 0$ (Table IV). Some IRs of C_{6v} are 2D, whereas all IRs of C_{2v} are 1D. Therefore, any double degeneracy when $\Delta n=0$ is removed, as Δn is varied. In fact, for any $\mathbf{k}$ vectors or any θ in hexagonal lattice, the $R_M(\mathbf{k})$ groups when $\Delta n\neq 0$ (Table IV) only have 1D IRs (Table X), and consequently all degeneracy, when $\Delta n=0$ is removed. However, we still need to be aware of accidental degeneracies due to the crossing of bands.

VI. CONCLUSION

This work has a fundamental impact in the design and the application of photonic crystals with anisotropic motifs. The work provides necessary group theoretical tools in identifying irreducible Brillouin zone, fundamental zone of motif's orientations, and the symmetries of the eigenmodes and eigenvalues of an anisotropic photonic crystal in the absence and presence of spatial modulation. The descriptions of IBZ, orientational group, and FZO of anisotropic PC are general and therefore can be applied for any 2D and 3D anisotropic PCs. On the other hand, the labeling states and the symmetry representations in the absence of presence of spatial modulation were illustrated by using a 2D anisotropic PC. Nevertheless, the labeling system and the analyses of symmetry representations can be extended for 3D anisotropic PCs as well.

ACKNOWLEDGMENT

G.A. thanks the Agency for Science, Technology and Research (A*STAR), Singapore for the support.

APPENDIX A

The free photon dispersion in a 2D hexagonal lattice is described by Eq. (20). For a 2D square lattice, the equation takes a similar form

$$\omega_{free}(\mathbf{k})=\frac{1}{n_y}\sqrt{c_1 m_{is}+c_2(r_n^2-1)m_{anis}+\omega_c}, \qquad \text{(A1)}$$

where the expressions for the constants c_1, c_2, and ω_c, and the discrete integers m_{is} and m_{anis} are listed in Table XII for the symmetrical points of a square lattice.

*exwsun@ntu.edu.sg

[1] S. John, Phys. Rev. Lett. **58**, 2486 (1987).
[2] E. Yablonovitch, Phys. Rev. Lett. **58**, 2059 (1987).
[3] T. F. Krauss, R. M. D. Rue, and S. Brand, Nature (London) **383**, 699 (1996).
[4] M. Notomi, Phys. Rev. B **62**, 10696 (2000).
[5] O. Painter, R. K. Lee, A. Scherer, A. Yariv, J. D. O'Brien, P. D. Dapkus, and I. Kim, Science **284**, 1819 (1999).
[6] P. V. Parimi, W. T. Lu, P. Vodo, and S. Sridhar, Nature (London) **426**, 404 (2003).
[7] A. Berrier, M. Mulot, M. Swillo, M. Qiu, L. Thylen, A. Talneau, and S. Anand, Phys. Rev. Lett. **93**, 073902 (2004).
[8] M. Qiu and S. He, Phys. Rev. B **60**, 10610 (1999).
[9] M. Agio and L. C. Andreani, Phys. Rev. B **61**, 15519 (2000).
[10] L. Shen, S. He, and S. Xiao, Phys. Rev. B **66**, 165315 (2002).
[11] X.-H. Wang, B.-Y. Gu, Z.-Y. Li, and G.-Z. Yang, Phys. Rev. B **60**, 11417 (1999).
[12] C. M. Anderson and K. P. Giapis, Phys. Rev. Lett. **77**, 2949 (1996).
[13] R. Wang, X.-H. Wang, B.-Y. Gu, and G.-Z. Yang, J. Appl. Phys. **90**, 4307 (2001).
[14] S. Kawakami, Electron. Lett. **33**, 1260 (1997).
[15] J. G. Fleming and S. Y. Lin, Opt. Lett. **24**, 49 (1999).
[16] D. Roundy and J. Joannopoulos, Appl. Phys. Lett. **82**, 3835 (2003).
[17] Z. Y. Li, B. Y. Gu, and G. Z. Yang, Phys. Rev. Lett. **81**, 2574 (1998).
[18] G. Alagappan, X. W. Sun, M. B. Yu, and P. Shum, J. Opt. Soc.

Am. B **23**, 1478 (2006).
[19] C. Y. Liu, Y. T. Peng, J. Z. Wang, and L. W. Chen, Physica B **388**, 124 (2004).
[20] Z. Y. Li, J. Wang, and B. Y. Gu, Phys. Rev. B **58**, 3721 (1998).
[21] K. Busch and S. John, Phys. Rev. Lett. **83**, 967 (1999).
[22] D. Kang, J. E. Maclennan, N. A. Clark, A. A. Zakhidov, and R. H. Baughman, Phys. Rev. Lett. **86**, 4052 (2001).
[23] H. Takeda and K. Yoshino, J. Appl. Phys. **92**, 5658 (2004).
[24] Y. Shimoda, M. Ozaki, and K. Yoshino, Appl. Phys. Lett. **79**, 3627 (2001).
[25] G. Alagappan, X. W. Sun, M. B. Yu, and P. Shum, IEEE J. Quantum Electron. **42**, 404 (2006).
[26] S. W. Leonard J. P. Mondia, H. M. vanDriel, O. Toader, S. John, K. Busch, A. Birner, U. Gosele, and V. Lehmann, Phys. Rev. B **61**, R2389 (2000).
[27] H. Takeda and K. Yoshino, Phys. Rev. E **67**, 056607 (2003).
[28] C.-Y. Liu and L.-W. Chen, Phys. Rev. B **72**, 045133 (2005).
[29] C. Schuller, F. Klopf, J. P. Reithmaier, M. Kamp, and A. Forchel, Appl. Phys. Lett. **82**, 2767 (2003).
[30] P. Halevi, J. A. Reyes-Avendaño, and J. A. Reyes-Cervantes, Phys. Rev. E **73**, 040701(R) (2006).
[31] H. Takeda and K. Yoshino, Phys. Rev. E **69**, 016605 (2004).
[32] L. P. Bouckaert, R. Smoluchowski, and E. Wigner, Phys. Rev. **50**, 58 (1936).
[33] S. L. Altmann, *Band Theory of Solids: An Introduction From The Point of View of Symmetry* (Oxford University Press, New York, 1991).
[34] K. Sakoda, Phys. Rev. B **52**, 7982 (1995).
[35] Z. Ruan, M. Qiu, S. Xiao, S. He, and L. Thylén, Phys. Rev. B **71**, 045111 (2005).
[36] A. Martínez, H. Míguez, A. Griol, and J. Martí, Phys. Rev. B **69**, 165119 (2004).
[37] K. Sakoda, *Optical Properties of Photonic Crystals* (Spinger, Berlin, 2001).
[38] D. Cassagne, C. Jouanin, and D. Bertho, Phys. Rev. B **53**, 7134 (1996).
[39] O. Painter and K. Srinivasan, Phys. Rev. B **68**, 035110 (2003).
[40] F. López-Tejeira, T. Ochiai, K. Sakoda, and J. Sánchez-Dehesa, Phys. Rev. B **65**, 195110 (2002).
[41] K. Sakoda, N. Kawai, T. Ito, A. Chutinan, S. Noda, T. Mitsuyu, and K. Hirao, Phys. Rev. B **64**, 045116 (2001).
[42] A. Ferrando, M. Zacarés, and M.-A. García-March, Phys. Rev. Lett. **95**, 043901 (2005).
[43] J. F. Cornwell, *Group Theory in Physics: An Introduction* (Acadamic, San Diego, 1997), Chap. 2, pp. 4, 5, and 7.
[44] T. Inui, Y. Tanabe, and Y. Onodera, *Group Theory and Its Application in Physics* (Springer, Berlin, 1996), Chaps. 2 and 4.
[45] K. Busch and S. John, Phys. Rev. E **58**, 3896 (1998).
[46] B. Bai and L. Li, J. Opt. Soc. Am. A **21**, 1886 (2004).
[47] W. Mao, Y. Zhong, J. Dong, and H. Wang, J. Opt. Soc. Am. B **22**, 1085 (2005).
[48] F. Pan, G. Knöpfle, Ch. Bosshard, S. Follonier, and R. Spreiter, Appl. Phys. Lett. **69**, 13 (1996).
[49] S. Gauza, C. H. Wen, S. T. Wu, N. Janarthanan, and C. S. Hsu, Jpn. J. Appl. Phys., Part 1 **43**, 7634 (2004).
[50] In order to verify Eq. (18), we start by considering the plane wave expansion of Eq. (3) for a general 3D problem. Such an expansion is given by Eq. (7) of Ref. 19 [for details, see the entire Sec. II of Ref. 19 or others (Refs. 31, 41, and 45)]. A vanishingly a small refractive index forces $\tilde{\varepsilon}^{-1}(\mathbf{r})=\Sigma_G\tilde{\varepsilon}^{-1}(\mathbf{G}) \approx \tilde{\varepsilon}^{-1}(0)=\mathrm{diag}(1/n_x^2,1/n_y^2,1/n_z^2)$ (Refs. 31 and 18) (i.e., assume the hole radius of 2D PC is very small and recall that $\theta=0$). Consequently, Eq. (7) of Ref. 19 will be diagonal with $\mathbf{G}=\mathbf{G}'$. In the (x,y,z) coordinate system with x-y being the 2D periodic plane $\mathbf{k}+\mathbf{G}$, can be written as $(k_x+G_x, k_y+G_y, 0)$ and further $\mathbf{e}_1$ is assumed to be pointing toward the z direction and $\mathbf{e}_2=\{\mathbf{e}_1 \times|\mathbf{k}+\mathbf{G}|\}/|\mathbf{k}+\mathbf{G}|$. Using these information and substituting in the plane wave expansion of Eq. (3) [i.e., Eq. (7) of Ref. 19] is straightforward to verify the dispersion relations in the absence of a spatial modulation for E and H polarizations. The dispersion relation for E and H polarizations is $(k_x+G_x)^2+(k_y+G_y)^2 =(2\pi n_z\omega/a)^2$, and Eq. (18), respectively, and further if the material is isotropic (i.e., $n_x=n_y=n_z$), it is easy to verify that the dispersion relation for E and H polarizations, is the same. In such, these relations correctly reproduce equations of circle at each (G_x,G_y) in Fig. 4(a) of Ref. 4.
[51] K.-M. Ho, C. T. Chan, and C. M. Soukoulis, Phys. Rev. Lett. **65**, 3152 (1990).
[52] W. Hergert and M. Dane, Phys. Status Solidi A **197**, 620 (2003).
[53] N. W. Ashcroft and N. D. Mermin, *Solid State Physics* (Thomson Learning, Inc., London, 1976).
[54] In group theory, the irreducible representation of a group is generally a reducible representation of its subgroup and called as a subduced representation. The subduced representation can be written as a sum of IRs of the subgroup by using the standard group theory reduction procedure. More detailed information can be found in any group theory textbooks (i.e., for example, Refs. 43 and 44).
[55] R. Moussa, S. Foteinopoulou, L. Zhang, G. Tuttle, K. Guven, E. Ozbay, and C. M. Soukoulis, Phys. Rev. B **71**, 085106 (2005).
[56] J. W. Haus, M. Siraj, P. Prasad, and P. Markowicz, Chin. Opt. Lett. **5**, 527 (2007).
[57] G. Alagappan, X. W. Sun, and M. B. Yu, Phys. Rev. B (to be published).
[58] G. Alagappan, X. W. Sun, M. B. Yu, and P. Shum, Phys. Rev. B **75**, 113104 (2007).